Plant Molecular Biology (2019) 100:181–197
https://doi.org/10.1007/s11103-019-00852-8

Engineering the acceptor substrate specificity in the xyloglucan endotransglycosylase TmXET6.3 from nasturtium seeds (*Tropaeolum majus* L.)

Barbora Stratilová[1,2] · Zuzana Firáková[1] · Jaroslav Klaudiny[1] · Sergej Šesták[1] · Stanislav Kozmon[1] · Dana Strouhalová[3] · Soňa Garajová[1] · Fairouz Ait-Mohand[1] · Ágnes Horváthová[1] · Vladimír Farkaš[1] · Eva Stratilová[1] · Maria Hrmova[4,5]

Received: 14 June 2018 / Accepted: 28 February 2019 / Published online: 13 March 2019

Abstract

Key message **The knowledge of substrate specificity of XET enzymes is important for the general understanding of metabolic pathways to challenge the established notion that these enzymes operate uniquely on cellulose-xyloglucan networks.**

Abstract Xyloglucan xyloglucosyl transferases (XETs) (EC 2.4.1.207) play a central role in loosening and re-arranging the cellulose-xyloglucan network, which is assumed to be the primary load-bearing structural component of plant cell walls. The sequence of mature TmXET6.3 from *Tropaeolum majus* (280 residues) was deduced by the nucleotide sequence analysis of complete cDNA by Rapid Amplification of cDNA Ends, based on tryptic and chymotryptic peptide sequences. Partly purified TmXET6.3, expressed in *Pichia* occurred in N-glycosylated and unglycosylated forms. The quantification of hetero-transglycosylation activities of TmXET6.3 revealed that (1,3;1,4)-, (1,6)- and (1,4)-β-D-glucooligosaccharides were the preferred acceptor substrates, while (1,4)-β-D-xylooligosaccharides, and arabinoxylo- and glucomanno-oligosaccharides were less preferred. The 3D model of TmXET6.3, and bioinformatics analyses of identified and putative plant xyloglucan endotransglycosylases (XETs)/hydrolases (XEHs) of the GH16 family revealed that H94, A104, Q108, K234 and K237 were the key residues that underpinned the acceptor substrate specificity of TmXET6.3. Compared to the wild-type enzyme, the single Q108R and K237T, and double-K234T/K237T and triple-H94Q/A104D/Q108R variants exhibited enhanced hetero-transglycosylation activities with xyloglucan and (1,4)-β-D-glucooligosaccharides, while those with (1,3;1,4)- and (1,6)-β-D-glucooligosaccharides were suppressed; the incorporation of xyloglucan to (1,4)-β-D-glucooligosaccharides by the H94Q variant was influenced most extensively. Structural and biochemical data of non-specific TmXET6.3 presented here extend the classic XET reaction mechanism by which these enzymes operate in plant cell walls. The evaluations of TmXET6.3 transglycosylation activities and the incidence of investigated residues in other members of the GH16 family suggest that a broad acceptor substrate specificity in plant XET enzymes could be more widespread than previously anticipated.

Keywords Bioinformatics · GH16 family · Homo- and hetero-transglycosylation · Protein molecular modelling · Site-directed mutagenesis

Barbora Stratilová and Zuzana Firáková have contributed equally to this work.

Database accession numbers: The nucleotide sequence of TmXET6.3 is available in GenBank under HF968473, the protein sequence of TmXET6.3 in UniprotKB under V5ZEF7, and the structural data of TmXET6.3 in the Protein Model DataBase under PM0081526.

Electronic supplementary material The online version of this article (https://doi.org/10.1007/s11103-019-00852-8) contains supplementary material, which is available to authorized users.

Extended author information available on the last page of the article

Abbreviations

2GalManO6-OS	2-galacto-manno-hexasaccharide
Ara-OS6	Arabino-heptasaccharide
AraGal-OS	Arabino-galacto-oligosaccharides
AraXyl-OS	Arabino-xylo-oligosaccharides
Cello-OS	Cello-oligosaccharides
Cello-OS3	Cello-triose
Cello-OS4	Cello-tetraose
Cello-OS5	Cello-pentaose
Cello-OS6	Cello-hexaose
CMC	Carboxymethyl cellulose
cpk	Atomic colour scheme

C'XET	TmXET6.3 without putative signal peptide
GalUA-OS5	Penta-galacturonic acid oligosaccharide
GalMan-OS	Galacto-manno-oligosaccharides
GlcMan-OS	Gluco-manno-oligosaccharides
GH16	Family 16 glycoside hydrolase
HEC	Hydroxyethyl cellulose
HPLC	High performance liquid chromatography
La	Laminarin
La-OS	Laminari-oligosaccharides
Man-OS	Manno-oligosaccharides
Man-OS6	Manno-hexa-oligosaccharide
MLG-OS	Mixed-linkage (1,3;1,4)-β-D-gluco-saccharides
MLG-OS4 A, B, C	(1,3;1,4)-β-D-tetra-glucosaccharides A, B, C
MALDI	Matrix-assisted laser desorption/ionisation
MS	Mass spectrometry
OS	Oligosaccharide(s)
Pu	Pustulan
Pu-OS	Pustulo-oligosaccharides
TmXET6.3	*Tropaeolum majus* XET6.3
RACE	Rapid Amplification of cDNA Ends
RMSD	Root-mean square deviation
SDS-PAGE	Sodium dodecyl sulfate–polyacrylamide gel electrophoresis
SR	Sulforhodamine
TOF	Time-of-flight
XEH	Xyloglucan endo-(1,4)-β-D-glucanase
XET/XTH	Xyloglucan endotransglycosylase/hydrolase
XG	Xyloglucan
XG-OS7	Xyloglucan heptasaccharide
XG-OS8	Xyloglucan octasaccharide
XG-OS9	Xyloglucan nonasaccharide
XG-OS	Xyloglucan oligosaccharides
Xyl	(1,4)-β-D-glucuronoxylan
Xyl-OS	(1,4)-β-D-glucurono-xylo-oligosaccharides
WT	Wild-type

Introduction

The main polysaccharide components of primary cell walls of dicotyledonous plants are cellulose, xyloglucans (XGs) and pectins (Farrokhi et al. 2006; Cosgrove 2014). XG polysaccharides constitute the polymers with four repeating (1,4)-β-D-linked glucopyranosyl subunits that are substituted at C-6 of glucopyranosyl moieties by xylosyl (α-D-Xyl*p*) substituents (Hayashi 1989; Fry et al. 1992; Farkaš et al. 1992). The XG polymer can further be galactosylated (β-D-Gal*p*-(1,2)-α-D-Xyl*p*) at C-2, and the galactosyl residues can be fucosylated (α-L-Fuc*p*-(1,2)-β-D-Gal*p*-(1,2)-α-D-Xyl*p*). Further, the arabinosyl substituents instead of the fucosyl residues (York et al. 1990, 1993), or the galactosyluronic acid substituents replacing the xylosyl moieties (Peña et al. 2012) were reported, supporting the view that the XG composition can vary from plant to plant (Vincken et al. 1997) or tissue to tissue (Peña et al. 2012). The unified nomenclature of the XG signature oligosaccharides (XG-OS), using one-letter codes was adopted to precisely define diverse XG compositions (Fry et al. 1993).

There is a broad structural similarity between XG and cellulose, which results in a conformational homology yielding strong non-covalent associations between cellulose and XG polysaccharides. Here, XG binds to the surface of cellulose microfibrils and is also inter-woven into the amorphous parts of cellulose microfibrils (Hayashi 1989). For this reason, the cellulose-XG network is regarded to be the main load-bearing structural component of plant primary cell walls, due to its strength and flexibility (Carpita and Gibeaut 1993; Chanliaud et al. 2002, 2004; Nishikubo et al. 2011; Park and Cosgrove 2015).

Plant growth is associated with re-organisation of cell walls, including loosening, elongation and expansion. The modification of saccharide components is mediated by enzymes enabling the cell wall to carry out its functions. XET enzymes are one of the key cell wall-associated enzymes that belong to the GH16 glycoside hydrolase family, based on the Carbohydrate Active Enzymes classification (http://www.cazy.org/GH16.html; CAZypedia Consortium 2018).

The XET activity was discovered independently by three research groups (Farkaš et al. 1992; Fry et al. 1992; Nishitani and Tominaga 1992). It was initially thought that XET enzymes catalyse both XEH and XET reactions (Chanliaud et al. 2004; De Silva et al. 1993; Fanutti et al. 1993, 1996; Schröder et al. 1998; Steele et al. 2001; Sulová et al. 2003; Lu et al. 2006). However, specific XEH and XET enzymes and dual specificity XET/XEH enzymes, forming the xyloglucan transferase/hydrolase (XTH) group, were later identified in a variety of plants, including poplar (Johansson et al. 2004; Baumann et al. 2007), barley (Hrmova et al. 2007, 2009) and nasturtium (Stratilová et al. 2010). While XET enzymes with the transferase activity (EC 2.4.1.207) catalyse cleavage of a 1,4-β-linked polyglucosyl XG chain and ligation of the formed reducing end-containing fragment to another molecule of XG (or polysaccharide), XEH or XG-specific endo-β-(1,4)-D-glucanases with the hydrolytic activity (EC 3.2.1.151) are responsible for an irreversible shortening of a XG chain (Rose et al. 2002). XTH enzymes are classified within three phylogenetic clades (Hrmova

et al. 2009); two of them include XET and a third one XEH enzymes. XET enzymes act by a ping-pong catalytic mechanism, where the association of the enzyme with a donor XG molecule is followed by the formation of a covalent glycosyl-enzyme complex intermediate and a release of the first-hydrolysed portion of the substrate. After the association of this intermediate with XG or XG-OS acceptor molecules, a transglycosylation reaction takes place that results in the formation of a covalent linkage between donor and acceptor molecules, followed by product dissociation and a free enzyme (Farkaš et al. 1992; Fry et al. 1992; Nishitani and Tominaga 1992; Baran et al. 2000).

Typically, several XET isoforms operate during plant development or in response to environmental stimuli, consequently the expression of *XTH* genes needs to be regulated (Schröder et al. 1998; Rose and Bennet 1999; Catalá et al. 2001; Atkinson et al. 2009; Muñoz-Bertomeu et al. 2013; Nardi et al. 2014). Owing to the XET catalytic mechanism, these enzymes are involved in the depolymerisation of polysaccharides and/or in a re-structuralisation of newly synthesised saccharides in cell walls. XET enzymes act primarily on XG molecules that later become associated with cellulose microfibrils thereby maintaining the cell wall integrity and ensuring the incorporation of newly formed XG molecules in plant cell walls (Johansson et al. 2004; Smith and Fry 1991; Thompson et al. 1997; Campbell and Braam 1999a, b; Thompson and Fry 2001). An increased expression of *XTH* genes is often associated with fruit ripening and softening, therefore XET enzymes not only strengthen, but also loosen cell walls facilitating further modification through cooperativity with other cell wall-associated enzymes (Rose and Bennet 1999; Redgwell and Fry 1993). Moreover, XET enzymes play key roles in the restructuring of primary cell walls, when secondary wall layers are deposited, most likely by generating and reinforcing the connections between primary and secondary cell wall layers (Bourquin et al. 2002). Experimental data illustrate irreplaceable roles of XET enzymes in saccharide metabolism associated with plant growth, and the increased secretion of saccharides during cell elongation that significantly influences properties of cell walls and tissues, as their shapes and sizes change (Farkaš et al. 1992; Fry et al. 1992; Nishitani and Tominaga 1992; Baran et al. 2000). The key factor determining whether XET strengthens or loosen cell walls is thought to be the amount of nascent XG present at a specific location of a cell wall (Nishikubo et al. 2011).

The plant cell wall is a complex cellular structure consisting of a cellulose-XG network, consisting of a broad spectrum of saccharide polymers, implying that a variety of enzymes and proteins could be involved in cell wall formation and decomposition. Thus, a question arises whether individual types of XET enzymes are strictly substrate-specific or could they also catalyse reactions with substrates that are different from XG?

In recent years, a new feature of XET enzymes has been unveiled. These enzymes catalyse so called hetero-transglycosylation reactions, using structurally different saccharides from XG as donor and acceptor substrates. Transglycosylating activities were found in protein extracts from nasturtium cotyledons (Ait-Mohand and Farkaš 2006) and barley seedlings (Hrmova et al. 2007, 2009), suggesting that these reactions may be wide-spread in plants. Glycosyl transfer reactions from XG to cello-oligosaccharides (Cello-OS) and laminari-oligosaccharides (La-OS), and from soluble cellulose derivates carboxymethyl cellulose (CMC) and hydroxyethylcellulose (HEC) to XG-OS, were revealed. Later, yet a broader in vitro substrate specificity of plant XET was described, transferring XG or HEC fragments to oligosaccharides (OS) derived from (1,4)-β-D-glucuronoxylan (Xyl), mixed-linkage (1,3;1,4)-D-β-glucan (MLG) and (1,6)-β-D-glucan (pustulan, Pu). These hetero-transglycosylation activities were assigned to HvXET5 (Hrmova et al. 2007) and HvXET6 (Hrmova et al. 2009), and nasturtium TmXET6.3 with the isoelectric point of 6.3 (Stratilová et al. 2010). In addition, HEC, CMC or Cello-OS were used as donors or acceptors with two partially purified XET isoforms from parsley (*Petroselinum crispum*) (Garajová et al. 2008).

Notably, the partial amino acid sequence of TmXET6.3, determined by matrix-assisted laser desorption/ionization time-of-flight (MALDI TOF/TOF) mass spectrometry revealed that TmXET6.3 differed from the previously described nasturtium XTH enzymes (Stratilová et al. 2010). Using polysaccharide microarrays in a high-throughput screening of transglycosylase activities, a broad substrate non-specificity of the nasturtium crude extracts was demonstrated (Kosík et al. 2010). Additional microscopic analyses were performed to test whether the unexpected glycosyl transfer from XG to yeast Pu-OS, took place in cell walls or elsewhere. Surprisingly, Pu-OS incorporation was primarily observed in a plasma membrane; this was most likely due to Pu-OS interacting with nascent cellulose chains synthesised in these locations (Zemková et al. 2012).

Furthermore, HEC, CMC and Cello-OS were used as donor and/or acceptor substrates with AtXTH3 from *Arabidopsis thaliana* (Shinohara et al. 2017), and Kosík et al. (2010) demonstrated with a crude *Arabidopsis* extract that XET enzymes transferred xylan fragments on XG-OS. Besides XET enzymes, other plant enzymes were identified to be transglycosylases that could covalently link various polysaccharides to XG (Fry et al. 2008; Mohler et al. 2013; Simmons et al. 2015; Simmons and Fry 2017). Further, mannan endotransglycosylase/ hydrolase was found to recognise (1,4)-β-D-mannan-derived polysaccharides (Schröder et al. 2006, 2009), while another enzyme was capable of endotransglycosylating heteroxylan polysaccharides

(Johnston et al. 2013). These studies demonstrated that plant transglycosylases exhibited a broad donor substrate specificity. These findings supported the assumption that these enzymes could link different polysaccharides in vivo, and have the potential to influence strength, porosity and flexibility of plant cell walls (Hrmova et al. 2007).

At the structural levels, X-ray diffraction studies of an XET enzyme from the hybrid aspen *Populus tremula x Populus tremuloides* (PttXET16A) (Johansson et al. 2004) revealed that this structure resembled to the other XTH enzymes in the GH16 family. Similarly, based on crystallographic analyses, XG endohydrolases TmNXG1 and TmNXG2 from *Tropaeolum majus*, exhibited typical structural features of the GH16 family enzymes (Baumann et al. 2007; Mark et al. 2009; McGregor et al. 2017). Even though TmNXG1 catalysed transglycosylation under the limited concentrations of an acceptor substrate, both PttXET16A and TmNXG1 catalysed the association of XG or HEC with XG-OS or water, respectively. This raises an important question of structural differences amongst non-specific XET enzymes of a diverse plant origin enabling them to operate on different donor and acceptor substrates.

Herein, we focus on the non-specific TmXET6.3 from germinated nasturtium seeds, primary structure of which was deduced from cDNA, and compare it to those of identified or predicted XET enzymes. The tertiary structural model of TmXET6.3 was constructed by homology modelling and residues responsible for the XET acceptor substrate specificity were identified. These data, corroborated with those obtained through site-directed mutagenesis, were combined with in vitro activity measurements, using structurally distinct donor and acceptor substrates.

Materials and methods

Protein extraction from plant materials

Nasturtium (*T. majus*) and parsley (*P. crispum*) seeds were planted or germinated on wet perlite under natural day/night regime at 22 °C. Nasturtium seedlings grown for 12 days were separated into seeds, roots, stems and leaves. Parsley seedlings germinated for seven days were separated into cotyledons with roots, and stems with leaves, whereas after seven days of parsley germination, only remnants of seeds were observed. Plant materials were homogenised (4 °C, 12 h) in 50 mM citrate–phosphate buffer, pH 6.0 containing 0.1 M imidazole and 1 M NaCl under shaking. The resultant materials were filtered through Miracloth (Calbiochem, USA) and centrifuged (20,000 × *g*, 20 min, 4 °C). Supernatants were precipitated to 90% saturation with solid ammonium sulfate for 24 h at 4 °C. The precipitated materials were centrifuged (20,000 × *g*, 20 min, 4 °C), the pellets dissolved in a small volume (10–20 mL) of distilled water, dialysed against distilled water for 24 h, and freeze-dried. Freeze-dried crude protein extracts were stored at − 20 °C until further use.

In situ microscopic analyses

Germinated nasturtium seeds were hand-sectioned. Enzyme activity was detected as described by Vissenberg et al. (2000), Nishikubo et al. (2007) and Ibatullin et al. (2009) with modifications as follows. Tissue sections were incubated in solutions containing 27.2 µM of sulforhodamine (SR)-labelled OS in 0.1 M succinate buffer, pH 5.5, for 1 h (XG-OS), and for 6 h (Cello-OS, MLG-OS, La-OS, Xyl-OS, Man-OS and GalUA-OS5) at ambient temperature (typically between 20 and 22 °C). The incorporation of OS into plant tissues was observed under the fluorescent microscope Nikon Eclipse 80i (CFI 15 × 40 CFI Plan Fluor), using 550 nm and 570 nm excitation and emission wavelengths, respectively, with images recorded using the DS-Fil Nikon camera (5-megapixel resolution).

RNA isolation

Nasturtium seeds were germinated on a wet perlite under natural day/night regime at an ambient temperature (18 to 22 °C) for seven days, subsequently frozen in liquid nitrogen and stored at − 80 °C. Frozen seeds were ground under liquid nitrogen using a mortar and a pestle. Tissue powders were transferred into pre-frozen microcentrifuge tubes (~ 80 mg per a tube) and homogenised in the lysis buffer containing 2 M NaCl using the ULTRA-TURRAX homogeniser (IKA Labortechnik, Germany). RNA was isolated following the protocol of the GeneJET^{TM} Plant RNA Purification Mini Kit (Thermo Scientific, USA). RNA isolated from around 400 mg of tissue was purified by the SiMax^{TM} Total RNA Columns Isolation kit (Ecoli, Slovakia) to remove DNA. The quality of prepared RNA was confirmed by 1.8% (w/v) agarose gel electrophoresis.

3′ and 5′ RACE

Rapid amplification of *TmXET6.3* cDNA ends was performed with the modified RACE procedure employing gene specific primers and a universal anchor-oligo(dT)-adaptor primer (AOdTA) (Frohman et al. 1998) (Supporting Table 1). The first, 3′ RACE was performed using a consensus-degenerate hybrid primer XETp1f as a specific primer for the polymerase chain reaction (PCR) amplification. The primer was designed according to the CODEHOP method (COnsensus-DEgenerate Hybrid Oligonucleotide Primer) (Rose et al. 1998) based on peptide sequences of TmXET6.3 (GNFNQDVDITWGDGR) and

the homologous to this peptide sequences of XTH21-ARATH from *Arabidopsis* and OsXTH12 from *Oryza sativa* (Stratilová et al. 2010). 5´ RACE was performed using specific primers for both cDNA synthesis (XET5RT) and PCR amplification (XET5amp). The primers were derived from the partial *TmXET6.3* cDNA sequence determined by 3´ RACE, as specified above.

The first strand cDNA ends were synthesised by the ReverAid™ Premium First Strand cDNA Synthesis Kit (Thermo Scientific, USA) from 1 µg of total RNA. Reverse transcriptions were performed according to the manufacturer´s recommendations using 50 pmol of AOdTA (3′ end) and 12.5 pmol of XET5RT (5′ end) primers in 20 µL reactions under the following conditions: 30 °C for 10 min, 50 °C for 30 min, 85 °C for 5 min (3′ end), and 50 °C for 30 min, 85 °C for 5 min (5′ end). The first cDNA strands from 5′ ends were purified with the High Pure PCR Product Purification Kit (Roche, Germany), whereby a portion of these strands (22 µL from the 50 µL of the purified sample) was dA-tailed with the Terminal Deoxynucleotidyl Transferase (Thermo Scientific, USA), followed by a 10-fold dilution in the 10 mM Tris–HCl buffer pH 8, containing 1 mM EDTA (Frohman et al. 1998).

PCR amplifications of cDNA ends were performed with the Phusion Hot Start II High-Fidelity DNA Polymerase (Thermo Scientific, USA), using 3 µL of 3´ and 4 µL of 5´ first strand cDNA samples in 50 µL volume reactions according to the manufacturer´s recommendations under the following regimes: the initial denaturation at 98 °C for 30 s, followed by 35 or 40 PCR cycles at 98 °C for 10 s, 64 °C for 30 s, and 72 °C for 30 s, with a final extension at 72 °C for 10 min.

Assembly of the *TmXET6.3* cDNA sequence

Fragments of *TmXET6.3* cDNAs with expected sizes obtained by 3′ and 5′ RACE, separated by 1.7% (w/v) agarose gel electrophoresis, were purified using the Wizard® SV Gel and the PCR Clean-Up System (Promega, USA), followed by ligation into the pJET1.2/blunt cloning vector (CloneJET PCR Cloning Kit, Thermo Scientific, USA). After transformation of *E. coli* XL10 Gold cells (Stratagene, USA), plasmids were isolated by the GeneJET™ Plasmid Miniprep Kit (Thermo Scientific, USA) from several clones and sequenced in both directions, employing the commercial service at the Comenius University (Bratislava, Slovakia). The sequence of complete *TmXET6.3* cDNA was assembled employing BioEdit (http://www.mbio.ncsu.edu/bioedit/bioedit.html). Protein sequence was predicted using Translator (http://www.justbio.com/) and the signal peptide using PrediSi (http://www.predisi.de/) and SignalP 4.0 (http://www.cbs.dtu.dk/services/SignalP-4.0/; Petersen et al. 2011).

Plasmid constructions for heterologous expression of TmXET6.3 and generation of variants

E. coli XL10-Gold cells (Agilent Technologies, Stockport, UK) were used throughout cloning. Standard protocols were used for plasmids constructions, *E. coli* transformation and plasmid preparation (Supporting Tables 2 and 3). To construct the pPICZα-His-FLAG-C'(G31)-XET DNA fusion, the region encoding truncated XET starting at G31 (C'XET) was amplified by PCR from the 3′ first strand cDNA, using the Phusion Hot Start II High-Fidelity DNA Polymerase (Thermo Scientific, USA), following the manufacturer's protocol. The PCR product was ligated into the pJET1.2/blunt plasmid producing pJET-C'XET (Supporting Table 2). To generate single H94Q, K237T and Q108R, and double K234T/K237T and tripple H94Q/A104D/Q108R variants, point mutations were introduced by the QuikChange site-directed mutagenesis kit, using the manufacturer protocol with pJET-C'XET specific primers (Supporting Table 3). The *Pml*I-*Xba*I fragments of pJET-H94Q-C'XET, pJET-Q108R-C'XET, pJET-K237T-C'XET, pJET-K234T/K237T-C'XET and pJET-H94Q/A104D/Q108R-C'XET were inserted into the *Pml*I- and *Xba*I-digested pPICZα-His-Flag vector (Supporting Table 2). PCR products and DNA fragments resulting from restriction digests were agarose gel-purified using the Wizard SV Gel and PCR Clean-Up System (Promega). All PCR-amplified sequences and sequences obtained by QuickChange site-directed mutagenesis (Agilent Technologies) were confirmed by automated Sanger sequencing in both directions. Plasmids were isolated using the QIAGEN Plasmid Midi Kit (Qiagen) and linearised by *Sac*I digestion before transformation into *P. pastoris*.

Expression of TmXET6.3 and its variants

P. pastoris strain GS115 was used as a host for the overexpression of truncated forms of XET and variants. *Pichia* was transformed by electroporation as described in the *Pichia* expression manual (Invitrogen). Transformants were selected on YPDS [1% (w/v) yeast extract, 2% (w/v) peptone, 2% (w/v) dextrose, 1M sorbitol] plates supplemented with zeocin (100 µg/ml) and screened for the XET activity in supernatants of small-scale experiments using methanol-containing MMYC medium [minimal medium with 0.5% (v/v) methanol and 1% (w/v) yeast extract, 2% (w/v) peptone, 1% (w/v) casamino acid] (Bencúrová et al. 2003) at 18 °C under shaking for four days. Crude or

partially purified culture media were used for analyses of hetero-transglycosylation activities.

Purification, deglycosylation and western immuno-blot of TmXET6.3

The medium with over-expressed TmXET6.3 (500 ml) was precipitated to 90% saturation with solid ammonium sulfate for 24 h at 4 °C and centrifuged (12,000x*g*, 20 min, 4 °C). The sediment dissolved in a small volume of distilled water was dialysed against 0.05 M phosphate buffer, pH 8.0 containing 0.3 M NaCl for 24 h at 4 °C and applied to the Bio-Scale™ Mini Nuvia™ Immobilised Metal Affinity Chromatography Ni-charged 5 ml Cartridge (Bio-Rad) connected to the NGC Discover Pro system (Bio-Rad). Fractions with XET activities were desalted using the Bio-Scale™ Mini Bio-Gel^R P-6 Desalting 10 ml Cartridge (Bio-Rad) and concentrated using the VivaSpin 500 centricon (Sartorius).

The purity of WT, and of the single H94Q, K237T and Q108R, and multiple K234T/K237T and H94Q/A104D/Q108R variants of TmXET6.3 was determined on 10% (w/v) SDS–PAGE gels (Laemmli 1970), using the Criterion Electrophoresis System (Bio-Rad Laboratories, Hercules, CA, USA). PageRuler™ Prestained Protein Ladder (Thermo Scientific) or Low Molecular Mass Standards (Sigma) were used as standards. Both Coomassie Brilliant Blue (PageBlue™ Protein Staining Solution, Thermo Scientific) and silver (Pierce Silver Stain for Mass Spectrometry, Thermo Scientific) staining protocols were used for protein visualisation on SDS–PAGE gels. Protein content was determined by the Qubit™ protein assay kit (Life Technologies, Carlsbad, CA, USA) using the Invitrogen Qubit fluorometer. Partially purified TmXET6.3 (Stratilová et al. 2010) was denatured by boiling for 5 min, cooled down and incubated with N-glycosidase F (Boehringer-Mannheim, Germany) in 0.1 M phosphate buffer, pH 7.0 at 37 °C for 72 h.

Western immuno-blot analyses were performed with SDS-PAGE-separated proteins transferred to polyvinylidene difluoride membranes with a pore size of 0.45 µm (AppliChem, Darmstadt, Germany) via an electro-transfer in the ice-cold 10 mM $NaHCO_3$ and 3 mM Na_2CO_3 buffer under stirring at 30 V overnight (Bio-Rad, CA, USA). Membranes were stained with 0.5% (w/v) Ponceau S in 1% (v/v) acetic acid for 5 min at ambient temperature of 18 to 22 °C and de-stained three times for two min in distilled water. Membranes were blocked overnight in the 5% (w/v) skimmed milk powder suspension in the PBST buffer [137 mM NaCl, 7 mM KCl, 101 mM Na_2HPO_4, 1.5 mM KH_2PO4, 0.1% (v/v) Tween 20] at 4 °C and incubated overnight at 4 °C with 1:1000 diluted mouse monoclonal anti-FLAG antibody (Sigma–Aldrich, St. Louis, MO, USA) in the PBST buffer containing the 5% (w/v) skimmed milk powder. Blots were washed four times in the PBST buffer and probed with the 1:20,000 diluted anti-Mouse IgG (H + L)-peroxidase conjugate (Thermo Scientific, Rockford, IL, USA) in the same buffer for 1 h at ambient temperature between 18 and 22 °C. Western immuno-blots were washed four times in the PBST buffer, developed by enhanced chemiluminescence (WesternBright™ ECL, Advansta Corp., CA, USA) and detected (ChemiDoc MP Imaging System, BioRad Laboratories, Hercules, CA, USA).

Substrates for enzyme reactions

Tamarind seed XG (molecular mass > 106 kDa) was kindly donated by Dr Mayumi Shirakawa (Dainippon Pharmaceutical Co., Ltd., Osaka, Japan), beechwood xylan was a gift from Dr Peter Biely (Institute of Chemistry of Slovak Academy of Sciences, Slovakia), powder cellulose (CE, fibers, medium) was purchased from Sigma, pustulan [Pu; (1,6) β-D-glucan] was supplied by Calbiochem (UK), barley MLG and wheat arabinoxylan were from Megazyme (Ireland), laminarin [La; (1,3)-β-D-glucan] and locust bean gum galactomannan (GalMan) were from Sigma (USA), and arabinogalactan (AraGal) was a gift from Dr Henk A. Schols (University of Wageningen, The Netherlands). Oligosaccharides (OS) derived from respective polysaccharides (XG-OS, Cello-OS, MLG-OS, Pu-OS, La-OS, Xyl-OS, AraXyl-OS, AraGal-OS, GalMan-OS) were prepared by the enzymic digestion of source polysaccharides as described (Kosík et al. 2010). Pentagalacturonic acid (GalUA-OS5) was a gift from Dr Anna Malovíková (Institute of Chemistry of Slovak Academy of Sciences, Slovakia). Arabinohexaose oligosaccharides (Ara-OS6), mannohexaose oligosaccharides (Man-OS6), 2-galactomannohexaose oligosaccharides (2GalMan-OS6), glucomannooligosaccharides (GlcMan-OS) and (1,3;1,4)-β-D-tetraglucooligosaccharides (MLG-OS4) with defined positions of (1,3)-linked glucosyl moieties A, B, C were purchased from Megazyme. Abbreviations, descriptions and chemical structures of all commercial and purified acceptor OS are defined in Scheme S1. OS were coupled with sulforhodamine (SR) as previously described (Kosík and Farkaš 2008). The purity of SR-labelled OS substrates was confirmed by thin-layer chromatography on silica gel plates (Merck) using the butan-1-ol:ethanol:water (5:3:2, by vol) solvent system. The chromatograms were viewed under a UV lamp. The molar concentrations of labelled OS were calculated based on the molar absorption coefficient for Lissamine rhodamine B sulphonyl chloride, $\varepsilon_{566} = 85{,}000\ M^{-1}\ cm^{-1}$ (Anaspec, CA, USA).

Enzyme activity assays

Nasturtium and parsley crude protein extracts or heterologously expressed WT and single and multiple variants of TmXET6.3 were used as an enzyme source. Enzyme activity

assays were performed by size-exclusion chromatography using the fluorimetric method, that utilises XG or other polysaccharides such as HEC, as donor substrates and SR-labelled OS as acceptor substrates. Reaction mixtures were incubated at 25 °C for different time intervals directly in vials placed in an autosampler of the HPLC (high-performance liquid chromatography) device (Dionex UltiMate 3000) with fluorescence and refractive index detectors. The analyses were performed through isocratic size-exclusion chromatography on the TSKgel G3000 SWXL column, 7.8 mm × 300 mm (TosoHaas, Tokyo, Japan), eluted with 100 mM ammonium acetate, pH 5.7 containing 20% (v/v) aqueous acetonitrile ($\phi_r = 0.2$) at a flow-rate 0.5 mL min^{-1}. The detector was programmed using respective 530 nm and 575 nm excitation and emission wavelengths. Chromeleon 6.80 software (Thermo Scientific, USA) was used for device control and data acquisition. All assays were performed in technical triplicates (n = 3) and activities with standard deviations were calculated via Excel in Microsoft Office Professional 2016.

Bioinformatics analyses

Homologous sequences to the TmXET6.3 protein sequence, were identified using BLAST and alignment tools of UniProtKB (http://www.uniprot.org). Protein sequence alignments were generated in Clustal Omega (Sievers et al. 2011). The evolutionary analysis of phylogenetic history was inferred using the Neighbor-Joining method (Saitou and Nei 1987) in Mega7 (Kumar et al. 2016). The evolutionary distances were computed using the p-distance method (Nei and Kumar 2000) and are expressed in the units of the number of amino acid residue differences per site. All positions containing gaps and missing data were eliminated.

3D Protein homology modelling

The homology model of TmXET6.3 was constructed based on the coordinates of the crystal structure of hybrid aspen PttXET16A as the template (Protein Data Bank ID: 1UN1; Johansson et al. 2004). This XET template was selected because of the mode of action, and higher sequence identity of TmXET6.1 to PttXET16A (41.5%) than that of TmXET6.3 to TmNXG1 (33.5%). Further, TmNXG1 is XEH rather than XET (Baumann et al. 2007). Homology models were generated in Modeller9v6 (Šali and Blundell 1993). Five models were generated with refined loops for each model. The best-scoring TmXET6.3 model was chosen based on the lowest probability density function and the lowest energy of loops. The root-mean-square-deviation (RMSD) values of Cα residues between TmXET6.3 and template structure 1UN1 were calculated using the cpptraj utility of AmberTools14 (Case et al. 2014). Superpositions between the TmXET6.3 homology model and the PttXET16A crystal structure revealed localisations of acceptor substrate sites.

Results and discussion

Localisation of non-specific XET enzymes in germinated nasturtium and parsley

The first XET enzyme with the hetero-transglycosylation activity was detected in germinated nasturtium seeds (Ait-Mohand and Farkaš 2006), although its precise localisation was uncertain. Later, Stratilová and co-workers (Stratilová et al. 2010) showed that only one non-specific TmXET6.3 isoform with hetero-transglycosylation activity occurred in seeds. To determine the precise localisation of XET enzymes with a hetero-transglycosylation activity in individual parts of nasturtium and parsley, we examined crude extracts of

Table 1 Hetero-transglycosylation activities of crude extracts of *T. majus* and *P. crispum*, with XG or HEC donor substrates and a variety of acceptor substrates. Abbreviations, descriptions and chemical structures of acceptor substrates are defined in Supporting Scheme 1

Activity						
Plant/tissues	XG-OS	Cello-OS	MLG-OS	La-OS	Xyl-OS	Pu-OS
T. majus/roots[a]	+	+	−	−	−	−
T. majus/stems[a]	+	+	−	−	−	−
T. majus/leaves[a]	+	+	−	−	−	−
T. majus/germinated seeds[b]	+	+	+	+	+	+
P. crispum/roots[c]	+	+	−	−	−	−
P. crispum/stems with leaves[a]	+	+	−	−	−	−
P. crispum/germinated seeds[a]	+	+	+	+	+	+

'+' or '−' presence or absence of hetero-transglycosylation activity

[a]Current work

[b]Stratilová et al. (2010)

[c]Garajová et al. (2008)

roots, stems and leaves separated from germinated seeds (Table 1) with SR-labelled XG-OS, Cello-OS, MLG-OS, La-OS, Xyl-OS and Pu-OS, defined in Scheme S1. These data indicated that crude extracts isolated from individual plant organs catalysed hetero-transglycosylation reactions with the following substrate pairs: XG/XG-OS, HEC/XG-OS, XG/Cello-OS and HEC/Cello-OS. Crude extracts from germinated seeds also contained enzymes that mediated hetero-transglycosylation reactions with XG or HEC as donors, and MLG-OS, La-OS, Xyl-OS and Pu-OS as acceptor substrates (Table 1).

Localisation of hetero-transglycosylation activities was investigated in germinated nasturtium seeds using SR-labelled XG-OS, La-OS, MLG-OS, Xyl-OS, Cello-OS, Man-OS and GalUA-OS5, as acceptors. SR-labelled La-OS, MLG-OS, Xyl-OS, Cello-OS integrated to the same structural regions of primary cell walls as those of XG-OS (Fig. 1). The only exceptions were SR-labelled Man-OS and GalUA-OS5, which did not show any specific cellular allocation.

It was previously documented that purified (Hrmova et al. 2007, 2009) or partially purified (Garajová et al. 2008; Shinohara et al. 2017) XET enzymes catalysed hetero-transglycosylation reactions with soluble cellulose derivatives HEC and CMC, as donor substrates and Cello-OS as acceptors. Conversely, Ruprecht et al. (2018), using crude stem extracts prepared from two-week-old nasturtium plants, did not detect the incorporation of fluorescently labelled XG-OS in HEC or xylan. The reason for the latter observations could be that, these authors did not test germinated nasturtium seed extracts, which is the source of non-specific XET enzymes (Stratilová et al. 2010).

Primary structure of non-specific TmXET6.3 and over-expression in P. pastoris

The primary structure of TmXET6.3 was determined using 3′ and 5′ RACE followed by cDNA sequencing, and by applying *de-novo* sequencing of tryptic and chymotryptic peptides of purified TmXET6.3 (Stratilová et al. 2010). Complete cDNA of TmXET6.3 (GenBank accession HF968473) consisted of 1078 bp without the poly(A) tail and contained an open reading frame encoding 280 amino acid residues (UniProtKB accession V5ZEF7) (Fig. 2). The

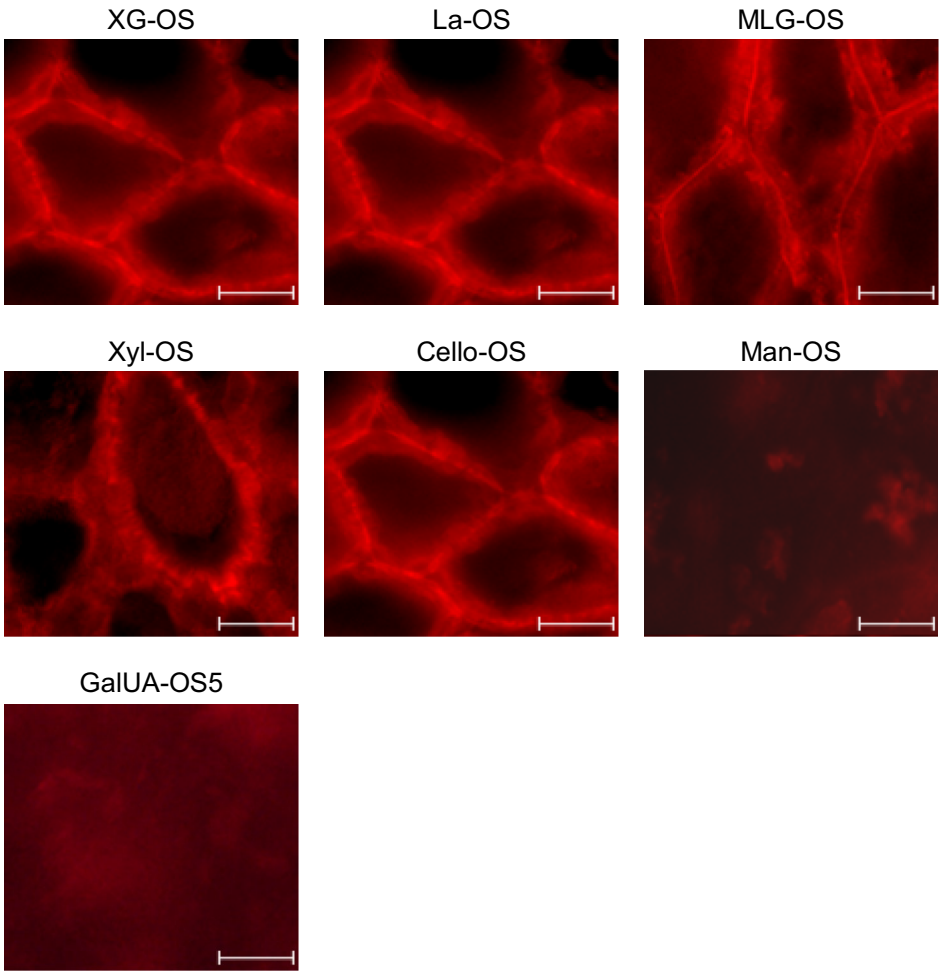

Fig. 1 Incorporation of the SR-labelled acceptor OS in the cell walls of germinated nasturtium seed. Germinated seeds were hand-sectioned, and enzyme activity detected as described in "Materials and methods". The panels with individual acceptor OS are specified. Scale bars correspond to 50 µm

```
ATT CTC ATA ATA TTG TAA AAA AGA ATT TGC CCA ATA ATA ATT ATG AAA ATA ATT TCT
                                                M   K   I   I   S
CGT TTT TCA ACA ATT ATT AAT ATT TTC TTA ATA ATT ATA TGT ATA ACT AGT TTA TCA
 R   F   S   T   I   I   N   I   F   L   I   I   I   C   I   T   S   L   S
TTT ACT ATA ATT TCT GCA GGT AAT TTT AAT CAA GAT GTC GAT ATT ACT TGG GGC GAT
 F   T   I   I   S   A   G   N   F   N   Q   D   V   D   I   T   W   G   D
GGT CGA GCT AAG ATA CTC GAC AAT GGC GAC CTT CTT ACT CTT TCA CTC GAT AAA GCT
 G   R   A   K   I   L   D   N   G   D   L   L   T   L   S   L   D   K   A
TCG GGG TCG GGT TTT CAA TCC AAA AAT GAA TAT ATT TTC GTA AAG ACT GAT ATG CAA
 S   G   S   G   F   Q   S   K   N   E   Y   I   F   V   K   T   D   M   Q
ATT AAA TTA ATC CAT GGT AAC TCG GCC GGT ACC GTT ACT ACG TCT TAC TTA CAA TCG
 I   K   L   I   H   G   N   S   A   G   T   V   T   T   S   Y   L   Q   S
AAA GGG GCT ACA TGG GAT GAA ATA GAT TTC GAA TTC TTA GGA AAC CTA AGT GGT GAT
 K   G   A   T   W   D   E   I   D   F   E   F   L   G   N   L   S   G   D
CCG TAC ATT GTT CAT ACA AAC ATT TTC GTT CAA GGA AAA GGT CGG AGA GAA CAA CAA
 P   Y   I   V   H   T   N   I   F   V   Q   G   K   G   A   R   E   Q   Q
TTC TAT CTT TGG TTT GAT CCA ACG ACA GAT TTC CAC ACT TAT TCC ATT ATT TGG AGT
 F   Y   L   W   F   D   P   T   T   D   F   H   T   Y   S   I   I   W   S
CCA CAA CAT ATA GTT TTA TTA GTT GAC AAC ATA CCA ATA AGA GAA TTC AAA AAC TTA
 P   Q   H   I   V   L   L   V   D   N   I   P   I   R   E   F   K   N   L
GAA TCC ATT GGA GTC CCA TAC CCA AAG TAT CAA CCC ATG AGA CTA CAA TGC ACA CTT
 E   S   I   G   V   P   Y   P   K   Y   Q   P   M   R   L   Q   C   T   L
TGG GAT GCT GAA GAT TGG GCT ACA AGA GGT GGT CAA GTA AAG ACT GAT TGG ACT CAA
 W   D   A   E   D   W   A   T   R   G   G   Q   V   K   T   D   W   T   Q
GCT CCT TTC ATT GCT TCT TAC AAA TAT TTC AAT GCT GAT ACA AAT AAG AAC CCT AGC
 A   P   F   I   A   S   Y   K   Y   F   N   A   D   T   N   K   N   P   S
ACT TCT ACT TGG TTT TCT CAA CAA TTG GAT TCT AAT AGC AAA GAA AAA CTC AAA TGG
 T   S   T   W   F   S   Q   Q   L   D   S   N   S   K   E   K   L   K   W
GTT CGA GAT AAT TAT ATG ATC TAT GAT TAT TGT AAA GAT TTT AAA CGA TTT TCA CAA
 V   R   D   N   Y   M   I   Y   D   Y   C   K   D   F   K   R   F   S   Q
GGA CTC CCT CGT GAA TGC AGT GTT AAT TGA TTA CTC AAT ATA ACC ATT ATA ATA AAT
 G   L   P   R   E   C   S   V   N
ATT TTT GAT AGT TAC TGC TAT CAA ATG GAT CTA TCA CTG ATC TAT GAT TAT TGT AAA
GAT TTT AAA CGA TTT TCA CAA GGA CTC CCT CGT GAA TGC AAT GTT AAT TGA TTA CTC
AAT ATA ACA ATT ATA ATA AAT ATT TTT GAT AGT TAT TGC TAT CAA ATG GAT CAA AAA
AAA AAA AAA AAA
```

Fig. 2 The nucleotide sequence of *TmXET6.3* mRNA (GenBank accession HF968473) and the primary structure of the TmXET6.3 translated protein (UniprotKB accession V5ZEF7). The signal peptide of 30 N-terminal residues (underlined) was predicted by PrediSi and SignalP 4.0. Two sets of mutated residues H94Q/A104D/Q108R and K234T/K237T (cf. Fig. 8) are labeled in respective black and grey boxes

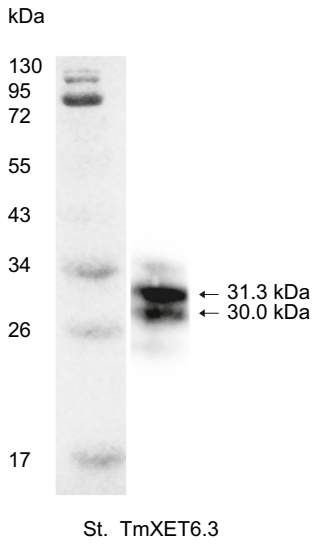

Fig. 3 Western immuno-blot of recombinant TmXET6.3, partially purified from the *P. pastoris* culture. The blot was detected via the immuno-reactive FLAG tag, as described in "Materials and methods". Two bands with arrows in the TmXET6.3 lane indicate the presence of full-length N-glycosylated (31.3 kDa) and unglycosylated (30.0 kDa) forms. Molecular mass standards (St.) are specified in kDa values

putative signal peptide was predicted to be 30 residues long with a cleavage site between Ala30 and Gly31 (Fig. 2).

The first strand cDNA was used as a template for cloning of cDNA encoding the mature form of TmXET6.3 (C'XET), lacking the putative signal peptide. The DNA construct with N-terminally fused 6xHis and FLAG tags and in-frame with C'XET was transformed in the *Pichia pastoris* host. The growth of methanol-induced *Pichia* cells was monitored by measurements of optical density and produced TmXET6.3 was detected by sodium dodecyl sulfate–polyacrylamide gel electrophoresis (SDS–PAGE) coupled with immuno-detection (Fig. 3) and enzymatic assays. Levels of the TmXET6.3 protein secreted into the medium were below the detection limits of Coomassie Brilliant Blue or silver staining methods. However, these preparations had a high specific activity, allowing us to use culture media for analyses of heterotransglycosylation activities.

Partial purification of *Pichia*-secreted TmXET6.3 was achieved by affinity purification on a Ni-binding resin, followed by desalting and freeze-drying of the protein. SDS–PAGE followed by staining did not detect protein bands in the preparation (Supporting Fig. 1), although western immuno-detection, based on the FLAG tag, visualised two major TmXET6.3 bands with molecular masses of 31.3 kDa and 30.0 kDa (Fig. 3). The smeared appearance of these bands suggested the presence of variously N-glycosylated and unglycosylated forms secreted to culture media. More precise inspection of unglycosylated TmXET6.3 indicated that it had molecular mass slightly below 30 kDa (Supporting Fig. 2). The mass difference of 1.3 kDa between the two forms is likely to correspond to around 8 hexosyl units at the N-glycosylation site N85 (motif NLS), following two catalytic residues E77 and E81 (residue numbering in TmXET6.3 is of that of lacking the 30-residue signal peptide—G31 is the starting residue; *cf.* Fig. 2). We further predicted the presence of seven O-glycosylation sites on S/T residues (Gupta 2001), although their occupancy remains to be confirmed. However, based on our previous findings with recombinant HvXET6 (Hrmova et al. 2009), TmXET6.3 could carry the EAEA NH_2-terminal extension sequence originating from the α-factor signal peptide, that is not properly processed (Raemaekers et al. 1999). In summary, based on our observations of unglycosylated TmXET6.3 purified from germinated seeds, we conclude that two major bands (Fig. 3) represented full-length N-glycosylated and unglycosylated forms, owing to micro-heterogeneity of nonuniform N- and O-glycosylation patterns. It is of note that in our hands unglycosylated TmXET6.3 due to N-deglycosylation lost its enzyme activity, so it is likely that N-glycosylation affects protein folding and/or catalytic activity. This confirms the observations (Roth et al. 2018) claiming that N- and O-glycosylation sites may affect protein stability, secretion and susceptibility to proteolytic degradation.

Hetero-transglycosylation activities and acceptor substrate specificity of TmXET6.3

The immuno dot-blot approach that uses a paper template and fluorescently labelled OS as acceptor substrates (Fry 1997; Kosík and Farkaš 2008) was unsuitable for testing hetero-transglycosylation activities, as acceptors such as Cello-OS, bind irreversibly to the paper template, thus hampering the evaluations of formed reaction products. For this reason, an HPLC inert size-exclusion chromatography column coupled to fluorescent or refractive index detectors was used. The suitability of this separation was first tested with XG as a donor that is recognised by the refractive index detector and later with XG-OS-SR as an acceptor monitored by a fluorescence detector. Here, transglycosylation activities were detected through the gradual increase of the intensity of fluorescence in the XG region, meaning that the enzyme activity could be evaluated directly from the integrated peak areas in a time-dependent manner (Fig. 4).

Recombinantly produced TmXET6.3 cleaved XG and HEC (data not shown) with different reaction rates and transferred saccharide fragments to a wide range of neutral SR-labelled OS (Scheme 1) composed of hexosyl or pentosyl residues linked by a diverse type of glycosidic linkages (Fig. 5a). We could not detect any hetero-transglycosylation activities with unfolded TmXET6.3 (via boiling) using all tested donor and acceptor substrates. A lower reaction rate was observed with SR-labelled 2-GalM6-OS and only negligible rates were detected with Man-OS and negatively charged GalUA-OS5 that corroborate the data in Fig. 1. With OS containing the mixed-type oligoglucoside-linked acceptor substrates, the TmXET6.3 activity depended on the distributions of these linkages (Fig. 5b), whereby the highest activity was observed with MLG-OS4 B (single 1,3-linkage is at the reducing end) and the lowest one with MLG-OS4 C (single penultimate 1,3-linkage is at the reducing end; *cf.* Scheme S1). Another factor influencing TmXET6.3 reaction rates was the oligosaccharide length of acceptor substrates (Fig. 5c). As expected, hetero-transglycosylation rates improved with increasing lengths of Cello-OS acceptors as previously noted with barley HvXET6 (Hrmova et al. 2009).

Comparative bioinformatics analyses, 3D homology modelling and TmXET6.3 variants design

In our previous work (Hrmova et al. 2009), the selected entries of the GH16 group were assembled into three distinct XTH groups I, II, III, based on primary structures that reflect their mode of action. Here, groups I and II cover entries with XET activities (the cleavage of a XG chain and ligation of the reducing end-containing fragment to another XG molecule or a polysaccharide), while group III contains enzymes with XEH activities (irreversible XG chain shortening due to hydrolysis). Based on the reconstruction of phylogeny of plant XET and other GH16 family members (Hrmova et al. 2009), non-specific TmXET6.3 was assigned to the XTH group II (Fig. 6a, green area). In this analysis we also included sequences of a non-plant origin, which are known as yeast polysaccharide cross-linkers. These enzymes are distantly related to XET/XTH entries, although these cross-linkers are phenomenologically similar to the other GH16 members (Hrmova et al. 2009). We anticipate that these

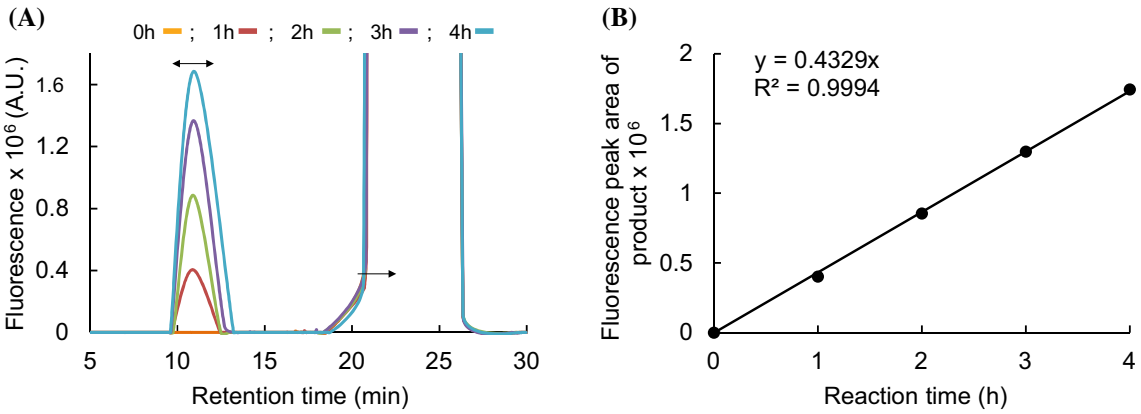

Fig. 4 Size-exclusion HPLC chromatography profile of transglycosylation reactions catalysed by TmXET6.3. **a** Synthesis of fluorescently labelled products (approximate average molecular masses between 60 and 100 kDa) was observed in a time-dependent manner (0, 1, 2, 3 and 4 h for brown-red, green, purple and blue lines, respectively), due to the incorporation of fluorescently labelled (1,3;1,4)-β-D-tetra-glucooligosaccharide MLG-OS4 C in high-molecular XG fragments. Respective double and single arrows indicate XG with incorporated SR-labelled MLG-OS4 C (retention time 10.8 min) and the SR-labelled MLG-OS4 C acceptor substrate (retention time 22.5 min). HPLC analyses were performed with refractive index and fluorescence detection. Chromeleon 6.80 software was used for peak area acquisitions. **b** Time-dependent evolution of fluorescent XG with MLG-OS4 C. Average data of three technical replicates (n = 3) are plotted with standard deviation values calculated via Excel in Microsoft Office Professional 2016

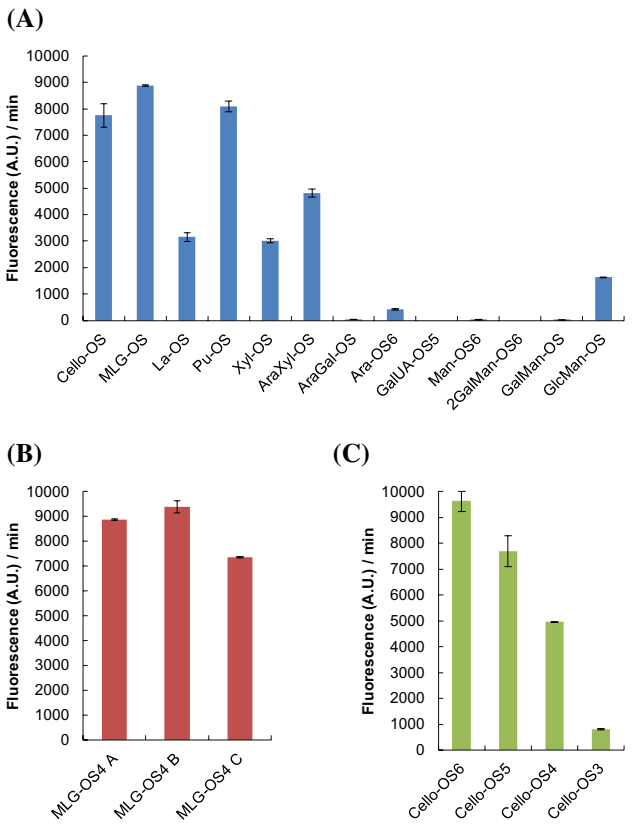

Fig. 5 Hetero-transglycosylation activities catalysed by TmXET6.3 were determined with chemically distinct SR-labelled acceptor OS. **a** Enzyme activities determined with a variety of acceptor OS. **b** Enzyme activities determined with (1,3;1,4)-β-D-tetraglucooligosaccharides MLG-OS4 A, MLG-OS4 B and MLG-OS4 C as the acceptors. **c** Enzyme activities determined with Cello-OS of degree of polymerisation 3–6 as the acceptors. XG was used in all cases as a donor substrate. Abbreviations, descriptions and chemical structures of acceptor OS are defined in Supporting Scheme 1. Average of three technical replicates (n = 3) are plotted with standard deviation values calculated via Excel in Microsoft Office Professional 2016

cross-linking enzymes could have similar spatial structures and catalyse hetero-transglycosylation reactions in yeast cell walls (Mazáň et al. 2013).

Further alignments of the TmXET6.3 sequence (V5ZEF7) with around 1000 UniprotKB proteins with at least 47% sequence identity indicated that all entries contained histidine in position 94, except for two entries with glutamine in corresponding positions (108), while 80% of XET entries carried the lysine residue in position 237. The fundamental problem with assigning the acceptor substrate specificity in these enzymes is in the absence of biochemical data; here unlike non-specific TmXET6.3, the substrate specific HvXET5 (P93668), TmXET1 (Q41614) and PttXET16 (Q8GZD5) belonging to GH16 group I (Fig. 6a, pink area), carry glutamine, arginine and a non-basic residue in these positions (Fig. 6b). These residues, which could potentially affect the substrate specificity of XET enzymes, were targeted for site-directed mutagenesis of TmXET6.3.

To understand the spatial distribution of key residues involved in catalysis and substrate specificity, we constructed the 3D homology model of TmXET6.3, based on the crystal structure of poplar PttXET16A as a template (Fig. 7). An excellent RMSD value of 0.227 Å was achieved between target and template structures indicating a close structural similarity of both proteins. As illustrated in the stereo projection (Fig. 7a), the differences in substrate specificity between TmXET6.3 and PttXET16A cannot be reconciled solely from spatial dispositions of these structures, although this information suggests the likely regions underlying this property (Fig. 7a). Nevertheless, this information revealed that at least two residues A104 and K234 might be important for enzyme interactions with acceptor substrates, in addition to H94, Q108 and K237 (Fig. 7b). Thus, through site-directed mutagenesis we replaced both K234 and K237 with the threonine residue (T) generating the K234T/K237T variant. Further, we have generated a triple H94Q/A104D/Q108R variant, with replacements of H94 for glutamine (Q), A104 for aspartic acid (D) and Q108 for arginine (R). While variations in a triple mutant collocated directly to the positions of β-sheet secondary structures, where the acceptor binding site is likely to be situated, K234T and K237T variations are located on a short loop in the proximity of the putative acceptor binding site (Fig. 7a). It is of note that positively charged K234 and K237 were replaced by non-conservative short neutral side chain residues, while the residues in the triple mutant were replaced more conservatively.

Comparisons of hetero-transglycosylation activities of H94Q, K237T and Q108R single and K234T/K237T and H94Q/A104D/Q108R multiple TmXET6.3 variants with the WT enzyme

We compared the enzyme activities of K234T/K237T double and H94Q/A104D/Q108R triple variants with those of WT TmXET6.3 (Fig. 8). Both variants exhibited a significantly increased activity with Cello-OS, relative to those with the natural XG-OS8 acceptor substrate in the following order: WT TmXET6.3 (0.8%) < K234T/K237T (2.6%) < H94Q/A104D/Q108R (4.8%) < crude nasturtium extract (7.6%). While K234T/K237T variants exhibited decreased relative activities on all investigated acceptor substrates (La-OS, MLG-OS, Pu-OS, Xyl-OS, AraXyl-OS and GlcMan-OS), except of Cello-OS6 (Fig. 8), even more significant effect of non-specificity suppression was observed in the triple H94Q/A104D/Q108R variant. Here, the pronounced decline to 2–4% of the original activity was observed, except of La-OS and Xyl-OS with the respective 50% and 33% declines. We therefore concluded that the key residue positions that may dictate an acceptor substrate specificity in XET enzymes

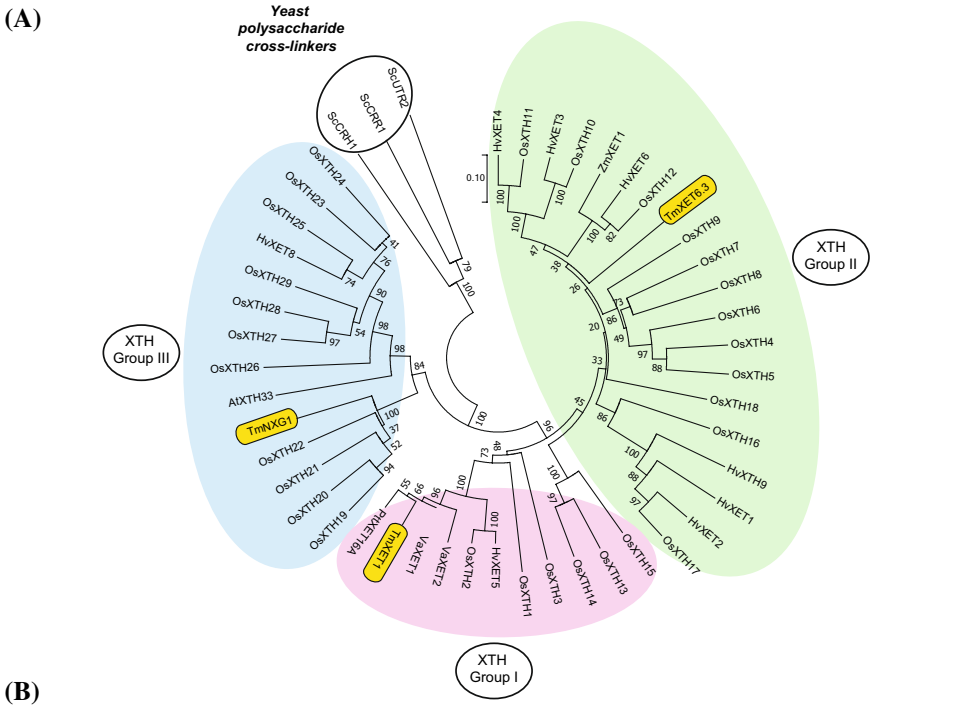

(B)

```
tr|P93668|      ------MKATAGALLAVVATVLLRGIAAAPPRKPVDVPFEKNYVPTWAEDHIHYVNGGRE
tr|Q41614|      -------MTSPKWFLFLGILVMATGAMGAAPKRPVAVPFGRNYAPTWAFDHIKYFNGGSD
tr|Q8GZD5|      ------MAAAYPWTLFLGMLVMVSGTMGAALRKPVDVAFGRNYVPTWAFDHIKYFNGGNE
tr|V5ZEF7|      MKIISRFSTIINIFLIIICITSLSFTIIS------AGNFNQDVDITWGDGRAKILDNGDL
                                :           :          * ::    **. .: : ...*
tr|P93668|      VQLSLDKTTGTGFQTRGSYLFGHFSMHIKLVGGDSAGTVTAFYLSSQNSEHDEIDFEFLG
tr|Q41614|      IQLHLDKYTGTGFQSKGSYLFGHFSMQIKLVPGDSAGTVTAFYLSSQNSEHDEIDFEFLG
tr|Q8GZD5|      IQLHLDKYTGTGFQSKGSYLFGHFSMQMKLVPGDSAGTVTAFYLSSQNSEHDEIDFEFLG
tr|V5ZEF7|      LTLSLDKASGSGFQSKNEYIFVKTDMQIKLIHGNSAGTVTTSYLQSKGATWDEIDFEFLG
                : * **: :*:***:..*:: : .*::**: *:*****:: **.*:.:  *********
tr|P93668|      NRTGQPYILQTNVFSGGKGDREQRIYLWFDPTKDYHSYSVLWNLYMIAFFVDDTPIRVFK
tr|Q41614|      NKTGQPYILQTNVFTGGKGDREQRIYLWFDPTKDYHSYSVLWNLYQIVFFVDDVPIRVFK
tr|Q8GZD5|      NRTGQPYILQTNVFTGGKGDREQRIYLWFDPTKEFHYYSVLWNMYMIVFLVDDVPIRVFK
tr|V5ZEF7|      NLSGDPYIVHTNIFVQGKGAREQQFYLWFDPTTDFHTYSIIWSPQHIVLLVDNIPIREFK
                * :*:** ::**::  *** ***:: :***** ::* **::*.   * : **. *** .:
tr|P93668|      NSK-DLGVRYPFDQPMKLYSSLWNADDWATRGGREKTDWSKAPFVASYRGFHVDGCEASA
tr|Q41614|      NSK-DLGVKFPFNQPMKIYSSLWNADDWATRGGLEKTDWSKAPFIASYKGFHVDGCEASV
tr|Q8GZD5|      NCK-DLGVKFPFNQPMKIYSSLWNADDWATRGGLEKTDWSKAPFIASYRSFHIDGCEASV
tr|V5ZEF7|      NLE-SIGVPYPKYQPMRLQCTLWDAEDWATRGGQVKTDWTQAPFIASYKYFNADTN----
                * :   ** :   * *:: .::*:*::***:**  :***::***:***: :  .
tr|P93668|      EAKLCATQGARWWDQPEFQDLDAAQYRRLAWVRKEHTIYNYCTDRERYAA-MSPECKRDRDV
tr|Q41614|      EAKFCATQGKRWWDQKEFQDLDGYQWRRLLWVRNKWTIYNYCNDRVRYPT-ISPECKRDRDI
tr|Q8GZD5|      EAKFCATQGARWWDQKEFQDLDAFQYRRLSWVRQKYTIYNYCTDRSRYPS-MPPECKRDRDI
tr|V5ZEF7|      ----KNPSTSTWF----SQQLDSNSKEKLKWVRDNYMIYDYCKDFKRFSQGLPRECSVN---
```

could be in the positions 94, 108 and 237 (residue numbering of TmXET6.3).

To compare the hetero-transglycosylation activities and impacts of individual substitutions with those of WT and multiple variants of TmXET6.3, we generated the single H94Q, Q108R and K237T variants. With SR-labelled Cello-OS as the acceptors, all single variants exhibited the increased hetero-transglycosylation activities with XG, when compared with the WT enzyme (Fig. 8). The most effective was H94Q, which incorporated the 6.2-fold higher amount of SR-labelled Cello-OS than WT; this represented about 81% the H94Q/A104D/Q108R activity, while the K237T variant exhibited 42% of the K234T/K237T activity emphasising the importance of the K234 residue.

As for the substrate specificity of single variants, Q108R could use all the tested SR-labelled MLG-OS, Pu-OS, Xyl-OS, AraXyl-OS, GlcMan-OS (Fig. 8), except La-OS, which only worked with H94Q/A104D/Q108R. In quantitative terms, the most pronounced decline of the hetero-transglycosylation activity was observed with Q108R with SR-labelled MLG-OS. Here, around a sevenfold decrease was observed compared to WT, while with other acceptors we detected a

Fig. 6 Phylogeny reconstruction of selected GH16 family members, and the multiple sequence alignment of TmXET6.3, TmXET1, HvXET5 and PttXET16, illustrating the conservation acceptor substrate specificity. **a** An unrooted radial phylogenetic tree of 48 GH16 members (including TmXET6.3 and TmXET1), sources of which were described in Hrmova et al. (2009). The optimal tree with the sum of branch length = 8.27 is shown. Bootstrap values for reproducibility out of 1000 trials are shown at the confluence of clusters. The tree is drawn to scale, with branch lengths in the same units as those of the evolutionary distances used to infer the tree. There was a total of 163 positions in the final dataset. Evolutionary analyses were conducted in MEGA7 (Kumar et al. 2016). **b** Acceptor substrate non-specific TmXET6.3 from germinated nasturtium seeds (UniProt accession V5ZEF7) and three acceptor substrate specific XET enzymes [TmXET1 (UniProt accession Q41614—from the overground parts of nasturtium), HvXET5 (P93668—from barley seedlings), PttXET16A (UniProt accession Q8GZD5—from poplar)] were aligned, using in Clustal Omega (Sievers et al. 2011). Putative residues responsible for non-specific and specific acceptor-binding are marked in respective black and grey boxes. Identical, highly similar and similar residues are marked by asterisks, colons and dots, respectively

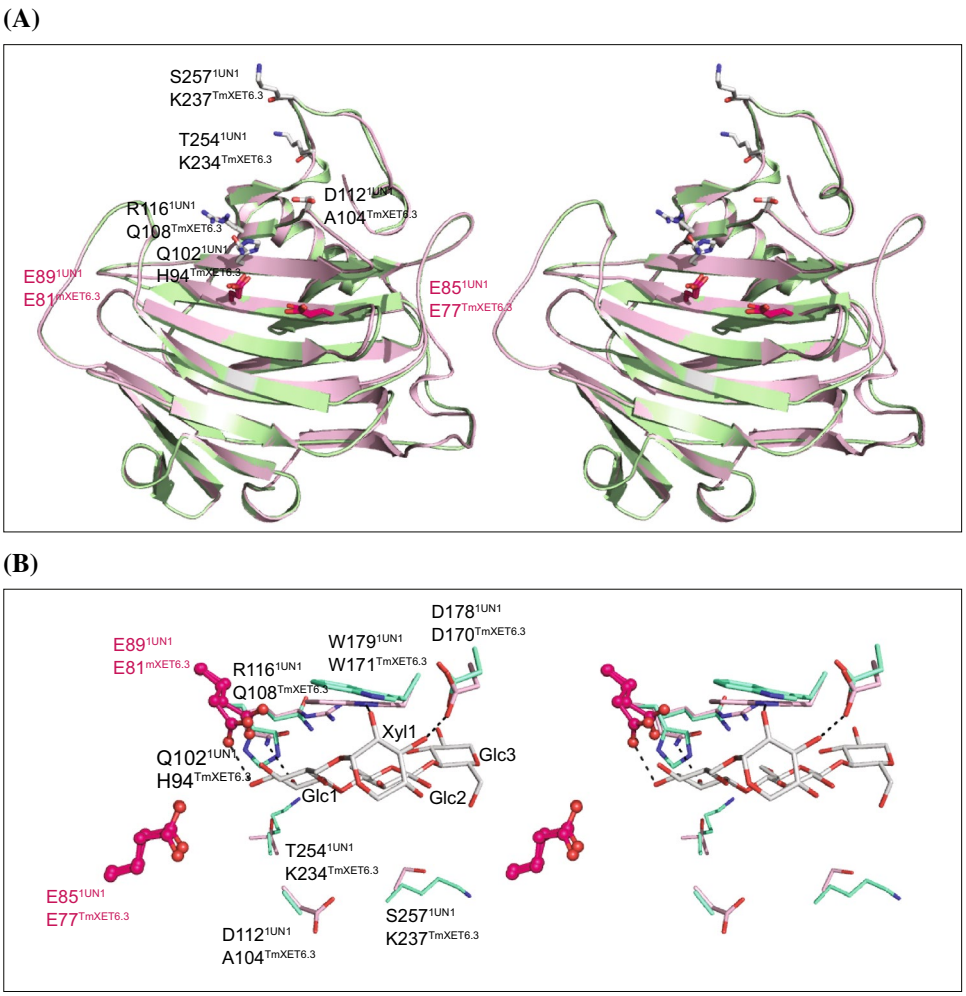

Fig. 7 Structural features of the TmXET6.3 homology model, superposed with the crystal structure of poplar PttXET16A. **a** Stereo projection of superposed TmXET6.3 (pale green) and PttXET16A (Protein Data Bank ID: 1UN1) (light pink) used as the template for modelling; the RMSD value of backbone residues between both structures is 0.227 Å. The cartoon illustrates the β-sandwich architecture with a jelly-roll topology, and catalytic (red cpk sticks) and five (cpk) putative residue pairs responsible for acceptor-binding specificity that were mutated in this work. **b** Stereo projection shows catalytic (sticks with spheres in cpk red) and mutated acceptor binding residues in PttXET16A (1UMZ) (light pink cpk sticks) and TmXET6.3 (green cpk sticks). Separations of 2.5–3.0 Å between residues and Glc1-Glc3 and Xyl1 moieties of the acceptor (cpk sticks) in PttXET16A are indicated in dashed lines. Residue numbering in TmXET6.3 is of that lacking the 30-residue signal peptide (G1 is the starting residue, cf. Fig. 2)

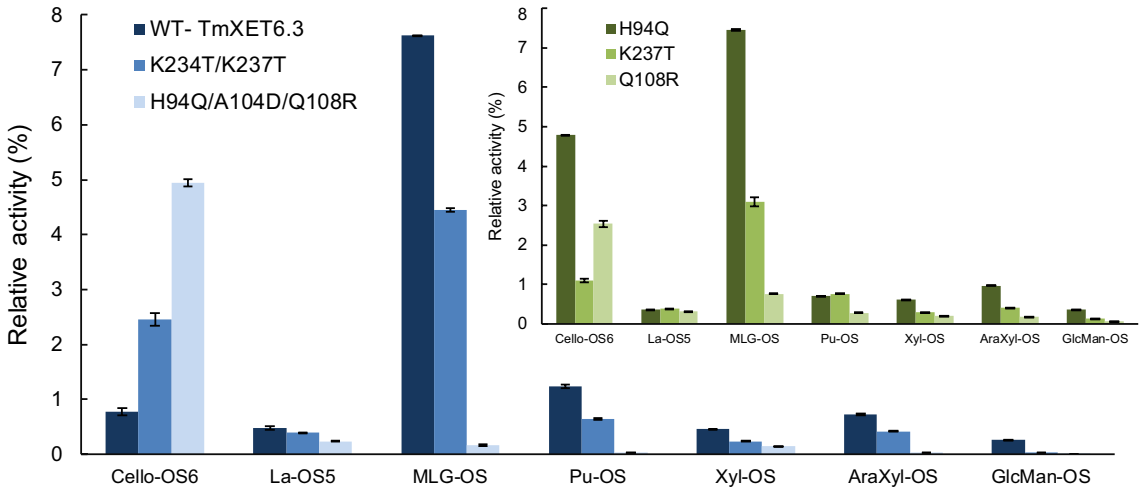

Fig. 8 Hetero-transglycosylation activities catalysed by TmXET6.3 (WT, wild-type), and its double K234T/K237T and triple H94Q/A104D/Q108R variants (inset with single H94Q, K237T and Q108R variants) were determined with XG as the donor substrate and a variety of chemically distinct SR-labelled acceptor OS. Abbreviations, descriptions and chemical structures of SR-labelled acceptor OS are defined in Scheme S1. Transglycosylation activities were normalised relative to 100% activity of the XG/XGO8 substrate pair. Average of three technical replicates (n = 3) are plotted with standard deviation values, calculated via Excel in Microsoft Office Professional 2016

2-3-fold decline (Fig. 8). We assume that the K237T change was responsible for the marked decline of hetero-transglycosylation observed with K234T/K237T (Fig. 8). Based on these findings we conclude that the Q108R and K237T residues might be the driving force behind the acceptor substrate preference, although residue variations in Q108R or K237T could also control this preference, although to a lesser extent.

While we observed suppression of the acceptor substrate specificity in variants, this observation was contrasted with a significant increase of their hetero-transglycosylation activities with Cello-OS6 (Fig. 8). Although Cello-OS seem to serve as convenient acceptors for specific (Hrmova et al. 2009) or non-specific (this work) XET enzymes, these acceptors were shown to be more effective with specific XET enzymes.

We envisage that biological roles of hetero-transglycosylation reactions catalysed by non-specific XET enzymes such as TmXET6.3 (Figs. 1, 4, 5, 8), might be in recognising many chemically distinct epitopes in cellular structures, including cell walls of germinating seeds. Using glycan-directed probes, heterogenous distribution of pectin and hemicellulose epitopes has been identified in the phloem cell walls of hardwood species (Kim and Daniel 2018), revealing that distributional patterns of these epitope varied between cell types and plant species. Similar epitope distributions may occur in nasturtium seed cell walls, where during the complex process of grain germination, non-specific XET enzymes could process many donor and acceptor substrate combinations. This possibility reinforces the concept that non-specific XET enzymes could create very large and continuous molecular networks within cell walls, and in vivo significantly alter their strength, flexibility, and porosity (Hrmova et al. 2007; Simmons and Fry 2017).

Large-scale bioinformatics analyses of XET entries

Multiple sequence alignments of XET entries, and H94, A104, Q108, K234 and K237 residue positions in TmXET6.3, and the corresponding positions in all available UniProtKB XET entries (3394) indicated the presence of H94, Q108 and K237 in 45, 148 and 352 respective cases, H94/Q108 in 372 cases, H94/Q108/K237 in 860 instances, H94/Q108/K234/K237 in 76 cases and H94/A104/Q108/K234/K237 in four instances (A0A067DUJ5_CITSI of *Citrus sinensis*, I1I5L3_BRADI of *Brachypodium distachyon*, V4UQR2_9ROSI of *Citrus clementina* and V5ZEF7_TROMA, that is TmXET6.3 of *T. majus*, described in this work), while the occurrence of specific XET enzymes with no variations in investigated residues was observed in 1537 cases (Fig. 9). These analyses clearly indicated that the XETs acceptor substrate non-specificity could be more widespread in plant XET enzymes than previously projected.

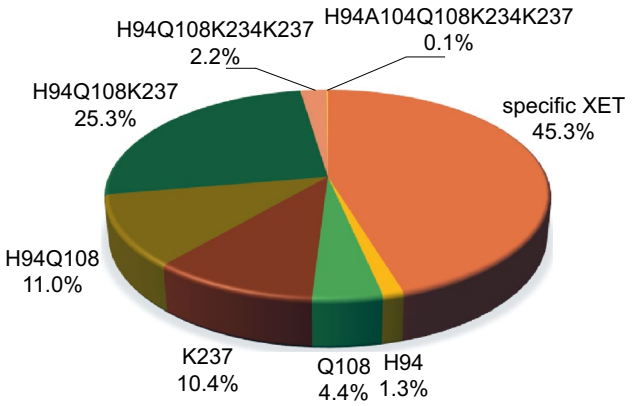

Fig. 9 Large-scale bioinformatics analysis of residue positions of available UniProtKB XET entries (3394) indicated the presence of H94, Q108 and K237 in 45 (1.3%), 148 (4.4%) and 352 (10.4%) respective cases, H94/Q108 in 372 cases (11.0%), H94/Q108/K237 in 860 instances (25.3%), H94/Q108/K234/K237 in 76 cases (2.2%) and H94/A104/Q108/K234/K237 in four instances (0.1%). The occurrence of specific XET enzymes with no variations in investigated residues was observed in 1537 cases (45.3%). One decimal point is given for each individual percentage

Based on the comparisons of the TmXET6.3 sequence with those of defined or putative XTH enzymes in the UniProtKB database, we predicted the importance of H94, A104, Q108, and K234 and K237 that could play the key importance in the acceptor substrate specificity of XET enzymes. These findings are supported by homology modelling of TmXET6.3, using the PttXET16A XET crystal structure as a template. Predictions of the significance of H94, A104, Q108, and K234 and K237 were tested in vitro through enzyme activity measurements of the variant enzymes prepared via site-directed mutagenesis. Bioinformatic analyses of known XTH enzymes classified in UniProtKB indicated that the broad XET acceptor substrate specificity could be more widespread among plant XET enzymes than it is often assumed. The knowledge of broad acceptor substrate specificity of TmXET6.3 could be useful for the general understanding of saccharide metabolic pathways, unlike the previously established notion that XET enzymes operate solely on cellulose-XG networks.

Acknowledgements This work was supported by the grant No. 2/0058/16 from VEGA, Slovakia to ES, and by the funding from Huaiyin Normal University and the Australian Research Council Linkage Project (DP120100900) to MH. We thank IBH Wilson from the Universität für Bodenkultur, Vienna, Austria, for providing the pPICZα-His/FLAG plasmid, to I Zelko and R Vadkertiova (Institute of Chemistry) for the assistance with fluorescent microscopy, and H Čigašová (Institute of Chemistry) for technical assistance.

Authors contributions Conceived, designed experiments and analysed data: B.S., Z.F., J.K., S.Š., E.S. and M.H. Z.F. and J.K. determined the primary structure of TmXET6.3, B.S. and E.S. quantified enzyme activities of wild-type and variants, Á.H., B.S. and F.A-M.

run electrophoretic analyses, E.S. conducted microscopy analyses, S.Š. constructed variant plasmids and selected hyper-producing clones, D.S. and S.G. worked out activity assays, S.K. built the 3D homology model, BS conducted large-scale bioinformatics analyses and suggested variant sites, V.F. prepared fluorescent oligosaccharides, M.H. conducted phylogeny reconstruction analyses and generated structural graphics. Discussed the data and contributed to writing: B.S., J.K., S.Š., S.K., V.F., E.S. and M.H. E.S. and M.H. designed research and wrote the manuscript.

Compliance with ethical standards

Conflict of interest Authors declare that they have no conflict of interest.

References

Ait-Mohand F, Farkaš V (2006) Screening for hetero-transglycosylating activities in extracts from nasturtium (*Tropaeolum majus*). Carbohydr Res 341:577–581. https://doi.org/10.1016/j.carres.2006.01.018

Atkinson RG, Johnston SL, Yauk Y-K, Sharma NN, Schröder R (2009) Analysis of xyloglucan endotransglucosylase/hydrolase (XTH) gene families in kiwifruit and apple. Postharvest Biol Technol 51:149–157. https://doi.org/10.1016/j.postharvbio.2008.06.014

Baran B, Sulová Z, Stratilová E, Farkaš V (2000) Ping-pong character of nasturtium-seed xyloglucan endotransglycosylase (XET) reaction. Gen Phys Biophys 19:427–440

Baumann MJ, Eklöf JM, Michel G, Kallas ÅM, Teeri TT, Czjzek M, Brumer H (2007) Structural evidence for the evolution of xyloglucanase activity from xyloglucan *endo*-transglycosylases: biological implications for cell wall metabolism. Plant Cell 19:1947–1963. https://doi.org/10.1105/tpc.107.051391

Bencúrová M, Rendić D, Fabini G, Kopecky EM, Altman F, Wilson IBH (2003) Expression of eukaryotic glycosyltransferases in the yeast *Pichia pastoris*. Biochimie 85:413–422. https://doi.org/10.1016/S0300-9084(03)00072-5

Bourquin V, Nishikubo N, Abe H, Brumer H, Denman S, Eklund M, Christiernin M, Teeri TT, Sundberg B, Mellerowicz EJ (2002) Xyloglucan endotransglycosylases have a function during the formation of secondary cell walls of vascular tissues. Plant Cell 14:3073–3088. https://doi.org/10.1105/tpc.007773

Campbell P, Braam J (1999a) *In vitro* activities of four xyloglucan endotransglycosylases from *Arabidopsis*. Plant J 18:371–382. https://doi.org/10.1046/j.1365-313X.1999.00459.x

Campbell P, Braam J (1999b) Xyloglucan endotransglycosylases: diversity of genes, enzymes and potential wall-modifying functions. Trends Plant Sci 4:361–366. https://doi.org/10.1016/S1360-1385(99)01468-5

Carpita NC, Gibeaut DM (1993) Structural models of primary cell walls in flowering plants: consistency of molecular structure with the physical properties of the walls during growth. Plant J 3:1–30. https://doi.org/10.1111/j.1365-313X.1993.tb00007.x

Case DA, Babin V, Berryman JT, Betz RM, Cai Q, Cerutti DS, Cheatham TE, Darden TA, Duke RE, Gohlke H et al (2014) AMBER 14. University of California, San Francisco

Catalá C, Rose JKC, York WS, Albersheim P, Darvill AG, Bennett AB (2001) Characterization of a tomato xyloglucan endotransglycosylase gene that is down-regulated by auxin in etiolated hypocotyls. Plant Phys 127:1180–1192. https://doi.org/10.1104/pp.010481

Chanliaud E, Burrows KM, Jeronimidis G, Gidley MJ (2002) Mechanical properties of primary plant cell wall analogues. Planta 215:989–996. https://doi.org/10.1007/s00425-002-0783-8

Chanliaud E, De Silva J, Strongitharm B, Jeronimidis G, Gidley MJ (2004) Mechanical effects of plant cell wall enzymes on cellulose/xyloglucan composites. Plant J 38:27–37. https://doi.org/10.1111/j.1365-313X.2004.02018.x

Cosgrove DJ (2014) Re-constructing our models of cellulose and primary cell wall assembly. Curr Opin Plant Biol 22:122–131. https://doi.org/10.1016/j.pbi.2014.11.001

De Silva J, Jarman CD, Arrowsmith DA, Stronach MS, Chengappa S, Sidebottom C, Reid JSG (1993) Molecular characterization of a xyloglucan-specific endo-(1→4)-β-D-glucanase (xyloglucan endotransglycosylase) from nasturtium seeds. Plant J 3:701–711. https://doi.org/10.1046/j.1365-313X.1993.03050701.x

Fanutti C, Gidley MJ, Reid JSG (1993) Action of a pure xyloglucan *endo*-transglycosylase (formerly called xyloglucan-specific *endo*-(1–4)-β-D-glucanase) from the cotyledons of germinated nasturtium seeds. Plant J 3:691–700. https://doi.org/10.1111/j.1365-313X.1993.00691.x

Fanutti C, Gidley MJ, Reid JSG (1996) Substrate subsite recognition of the xyloglucan endo-transglycosylase or xyloglucan-specific endo-(1→)-β-D-glucanase from the cotyledons of germinated nasturtium (*Tropaeolum majus* L.) seeds. Planta 200:221–228. https://doi.org/10.1007/BF00208312

Farkaš V, Sulová Z, Stratilová E, Hanna R, Maclachlan G (1992) Cleavage of xyloglucan by nasturtium seed xyloglucanase and transglycosylation to xyloglucan subunit oligosaccharides. Arch Biochem Biophys 298:365–370. https://doi.org/10.1016/0003-9861(92)90423-T

Farrokhi N, Burton RA, Brownfield L, Hrmova M, Wilson SM, Bacic A, Fincher GB (2006) Plant cell wall biosynthesis: genetic, biochemical and functional genomics approaches to the identification of key genes. Plant Biotechnol J 4:145–167. https://doi.org/10.1111/j.1467-7652.2005.00169.x

Frohman MA, Dush MK, Martin GR (1998) Rapid production of full-lenght cDNAs from rare transcripts: amplification using a single gene-specific oligonucleotide primer. Proc Natl Acad Sci USA 85:8998–9002. https://doi.org/10.1073/pnas.85.23.8998

Fry SC (1997) Novel "dot-blot" assays for glycosyltransferases and glycosylhydrolases: optimization for xyloglucan endotransglycosylase (XET) activity. Plant J 11:1141–1150. https://doi.org/10.1046/j.1365-313X.1997.11051141.x

Fry SC, Smith RC, Renwick KF, Martin DJ, Hodge SK, Matthews KJ (1992) Xyloglucan endotransglycosylase, a new wall-loosening enzyme activity from plants. Biochem J 282:821–828. https://doi.org/10.1042/bj2820821

Fry SC, York WS, Albersheim P, Darvill A, Hayashi T, Joseleau J-P, Kato Y, Lorences EP, Maclachlan GA, McNeil M (1993) An unambiguous nomenclature for xyloglucan-derived oligosaccharides. Physiol Plant 89:1–3. https://doi.org/10.1111/j.1399-3054.1993.tb01778.x

Fry SC, Mohler KE, Nesselrode BHWA, Franková L (2008) Mixed-linkage β-glucan: xyloglucan endotransglucosylase, a novel wall-remodelling enzyme from *Equisetum* (horsetails) and charophytic algae. Plant J 55:240–252. https://doi.org/10.1111/j.1365-313X.2008.03504.x

Garajová S, Flodrová D, Ait-Mohand F, Farkaš V, Stratilová E (2008) Characterization of two partially purified xyloglucan endotransglycosylases from parsley (*Petroselinum crispum*) roots. Biologia 63:313–319. https://doi.org/10.2478/s11756-008-0067-2

Gupta R (2001) Prediction of glycosylation sites in proteomes: from post-translational modifications to protein function. Dissertation, DTU Bioinformatics, Denmark

Hayashi T (1989) Xyloglucans in the primary cell wall. Annu Rev Plant Physiol Plant Mol Biol 40:139–168. https://doi.org/10.1146/annurev.pp.40.060189.001035

Hrmova M, Farkaš V, Lahnstein J, Fincher GB (2007) A Barley xyloglucan xyloglucosyl transferase covalently links xyloglucan, cellulosic substrates, and (1,3;1,4)-β-D-glucans. J Biol Chem 282:12951–12962. https://doi.org/10.1074/jbc.M611487200

Hrmova M, Farkaš V, Harvey AJ, Lahnstein J, Wischmann B, Kaewthai N, Ezcurra I, Teeri TT, Fincher GB (2009) Substrate specificity and catalytic mechanism of a xyloglucan xyloglucosyl transferase HvXET6 from barley (*Hordeum vulgare* L.). FEBS J 276:437–456. https://doi.org/10.1111/j.1742-4658.2008.06791.x

Ibatullin FM, Banasiak A, Baumann MJ, Greffe L, Takahashi J, Mellerowicz EJ, Brumer H (2009) A Real-time fluorogenic assay for the visualization of glycoside hydrolase activity in planta. Plant Phys 151:1741–1750. https://doi.org/10.1104/pp.109.147439

Johansson P, Brumer H 3rd, Baumann MJ, Kallas AM, Henriksson H, Denman SE, Teeri TT, Jones TA (2004) Crystal structures of a poplar xyloglucan endotransglycosylase reveal details of transglycosylation acceptor binding. Plant Cell 16:874–886. https://doi.org/10.1105/tpc.020065

Johnston S, Prakash R, Chen NJ, Kumagai MH, Turano HM, Cooney JM, Atkinson RG, Paull RE, Cheetamun R, Bacic A et al (2013) An enzyme activity capable of endotransglycosylation of heteroxylan polysaccharides is present in plant primary cell walls. Planta 237:173–187. https://doi.org/10.1007/s00425-012-1766-z

Kim JS, Daniel G (2018) Heterogenous distribution of pectin and hemicellulose epitopes in the phloem of four hardwood species. Trees 32:393–414. https://doi.org/10.1007/s0046

Kosík O, Farkaš V (2008) One-pot synthesis of xyloglucan oligosaccharides fluorescently labeled with sulforhodamine. Anal Biochem 375:232–236. https://doi.org/10.1016/j.ab.2007.11.025

Kosík O, Auburn RP, Russel S, Stratilová E, Garajová S, Hrmova M, Farkaš V (2010) Polysaccharide microarrays for high-throughput screening of transglycosylase activities in plant extracts. Glycoconj J 27:79–87. https://doi.org/10.1007/s10719-009-9271-8

Kumar S, Stecher G, Tamura K (2016) MEGA7: Molecular Evolutionary Genetics Analysis version 7.0 for bigger datasets. Mol Biol Evol 33:1870–1874. https://doi.org/10.1093/molbev/msw054

Laemmli UK (1970) Cleavage of structural proteins during the assembly of the head of bacteriophage T4. Nature 227:680–685. https://doi.org/10.1038/227680a0

Lu W, Wang Y, Jiang Y, Li J, Liu H, Duan X, Song L (2006) Differential expression of litchi XET genes in relation to fruit growth. Plant Phys Biochem 44:707–713. https://doi.org/10.1016/j.plaphy.2006.09.020

Mark P, Baumann MJ, Eklöf JM, Gullfot F, Michel G, Kallas ÅM, Teeri TT, Brumer H, Czjzek M (2009) Analysis of nastrutium *Tm*NXG1 complexes by crystallography and molecular dynamics provides detailed insight into substrate recognition by family GH16 xyloglucan *endo*-transglycosylases and *endo*-hydrolases. Proteins 75:820–836. https://doi.org/10.1002/prot.22291

Mazáň M, Blanco N, Kováčová K, Firáková Z, Řehulka P, Farkaš V, Arroyo J (2013) A novel fluorescence assay and catalytic properties of Crh1 and Crh2 yeast cell wall transglycosylases. Biochem J 455:307–318. https://doi.org/10.1042/BJ20130354

McGregor N, Yin V, Tung ChCh, Van Petegem F, Brumer H (2017) Crystallographic insight into the evolutionary origins of xyloglucan endotransglycosylases and endohydrolases. Plant J 89:651–670. https://doi.org/10.1111/tpj.13421

Mohler KE, Simmons TJ, Fry SC (2013) Mixed-linkage glucan:xyloglucan endotransglucosylase (MXE) re-models hemicelluloses in *Equisetum* shoots but not in barley shoots or *Equisetum* callus. New Phytol 197:111–122. https://doi.org/10.1111/j.1469-8137.2012.04371.x

Muñoz-Bertomeu J, Miedes E, Lorences EP (2013) Expression of xyloglucan endotransglucosylase/hydrolase (*XTH*) genes and XET activity in ethylene treated apple and tomato fruits. J Plant Phys 170:1194–1201. https://doi.org/10.1016/j.jplph.2013.03.015

Nardi CF, Villarreal NM, Opazo MC, Martínez GA, Moya-León MA, Civello PM (2014) Expression of *FaXTH1* and *FaXTH2* genes in strawberry fruit. Cloning of promoter regions and effect of plant growth regulators. Sci Hortic 165:111–122. https://doi.org/10.1016/j.scienta.2013.10.035

Nei M, Kumar S (2000) Molecular evolution and phylogenetics. Oxford University Press, New York. https://doi.org/10.1046/j.1365-2540.2001.0923a.x

Nishikubo N, Awano T, Banasiak A, Bourquin V, Ibatullin F, Funada R, Brumer H, Teeri TT, Hayashi T, Sundberg B, Mellerowicz EJ (2007) Xyloglucan endo-transglycosylase (XET) functions in gelatinous layers of tension wood fibers in poplar—a glimpse into the mechanism of the balancing act of trees. Plant Cell Phys 48:843–855. https://doi.org/10.1093/pcp/pcm055

Nishikubo N, Takahashi J, Roos AA, Derba-Maceluch M, Piens K, Brumer H, Teeri TT, Stålbrand H, Mellerowicz EJ (2011) Xyloglucan *endo*-transglycosylase-mediated xyloglucan rearrangements in developing wood of hybrid aspen. Plant Phys 155:399–413. https://doi.org/10.1104/pp.110.166934

Nishitani K, Tominaga R (1992) Endo-xyloglucan transferase, a novel class of glycosyltransferase that catalyzes transfer of a segment of xyloglucan molecule to another xyloglucan molecule. J Biol Chem 267:21058–21064

Park YB, Cosgrove DJ (2015) Xyloglucan and its interactions with other components of the growing cell wall. Plant Cell Phys 56:180–194. https://doi.org/10.1093/pcp/pcu204

Peña MJ, Kong Y, York WS, O'Neill MA (2012) A galacturonic acid-containing xyloglucan is involved in *Arabidopsis* root hair tip growth. Plant Cell 24:4511–4524. https://doi.org/10.1105/tpc.112.103390

Petersen TN, Brunak S, von Heijne G, Nielsen H (2011) SignalP 4.0: discriminating signal peptides from transmembrane regions. Nat Methods 8:785–786. https://doi.org/10.1038/nmeth.1701

Raemaekers R, de Muro L, Gatehouse JA, Fordham-Skelton AP (1999) Functional phytohemagglutinin (PHA) and *Galanthus nivalis* agglutinin (GNA) expressed in *Pichia pastoris*. Eur J Biochem 265:394–403. https://doi.org/10.1046/j.1432-1327.1999.00749.x

Redgwell RJ, Fry SC (1993) Xyloglucan endotransglycosylase activity increases during kiwifruit (*Actinidia deliciosa*) ripening (implications for fruit softening). Plant Phys 103:1399–1406. https://doi.org/10.1104/pp.103.4.1399

Rose JKC, Bennet AB (1999) Cooperative disassembly of the cellulose–xyloglucan network of plant cell walls: parallels between cell expansion and fruit ripening. Trends Plant Sci 4:176–183. https://doi.org/10.1016/S1360-1385(99)01405-3

Rose TM, Schultz ER, Henikoff JG, Pietrokovski S, McCallum CM, Henikoff S (1998) Consensus-degenerate hybrid oligonucleotide primers for amplification of distantly related sequences. Nucleic Acids Res 26:1628–1635. https://doi.org/10.1093/nar/26.7.1628

Rose JKC, Braam J, Fry SC, Nishitani K (2002) The XTH family of enzymes involved in xyloglucan endotransglucosylation and endohydrolysis: current perspectives and a new unifying nomenclature. Plant Cell Phys 43:1421–1435. 10.1093%2Fpcp%2Fpcf171

Roth C, Moroz OV, Ariza A, Skov LK, Ayabe K, Davies GJ, Wilson KS (2018) Structural insight into industrially-relevant glucoamylases: flexible positions of starch-binding domains. Acta Crystallogr D 74:463–470. https://doi.org/10.1107/S2059798318004989

Ruprecht C, Dallabernardina P, Smith PJ, Urbanowicz BR, Pfrengle F (2018) Analyzing Xyloglucan endotransglycosylases by incorporating synthetic oligosaccharides into plant cell walls. ChemBioChem 19:793–798. https://doi.org/10.1002/cbic.201700638

Saitou N, Nei M (1987) The Neighbor-Joining method: A new method for reconstructing phylogenetic trees. Mol Biol Evol 4:406–425. https://doi.org/10.1093/oxfordjournals.molbev.a040454

Šali A, Blundell TL (1993) Comparative protein modelling by satisfaction of spatial restraints. J Mol Biol 234:779–815. https://doi.org/10.1006/jmbi.1993.1626

Schröder R, Atkinson RG, Langenkämper G, Redgwell RJ (1998) Biochemical and molecular characterization of xyloglucan endotransglycosylase from ripe kiwifruit. Planta 204:242–251. https://doi.org/10.1007/s004250050253

Schröder R, Wegrzyn TF, Sharma NN, Atkinson RG (2006) LeMAN4 endo-beta-mannanase from ripe tomato fruit can act as a mannan transglycosylase or hydrolase. Planta 224:1091–1102. https://doi.org/10.1007/s00425-006-0286-0

Schröder R, Atkinson RG, Redgwell RJ (2009) Re-interpreting the role of endo-β-mannanases as mannan endotransglycosylase/hydrolases in the plant cell wall. Ann Bot 104:197–204. https://doi.org/10.1093/aob/mcp120

Shinohara N, Sunagawa N, Tamura S, Yokoyama R, Ueda M, Igarashi K, Nishitani K (2017) The plant cell-wall enzyme AtXTH3 catalyses covalent cross-linking between cellulose and cellooligosaccharide. Sci Rep 7:46099. https://doi.org/10.1038/srep46099

Sievers F, Wilm A, Dineen DG, Gibson TJ, Karplus K, Li W, Lopez R, McWilliam H, Remmert M, Söding J, Thompson JD, Higgins DG (2011) Fast, scalable generation of high-quality protein multiple sequence alignments using Clustal Omega. Mol Syst Biol 7:539. https://doi.org/10.1038/msb.2011.75

Simmons TJ, Fry SC (2017) Bonds broken and formed during the mixed-linkage glucan: xyloglucan endotransglucosylase reaction catalysed by *Equisetum* hetero-trans-β-glucanase. Biochem J 474:1055–1070. https://doi.org/10.1042/BCJ20160935

Simmons TJ, Mohler KE, Holland C, Goubet F, Franková L, Houston DR, Hudson AD, Meulewaeter F, Fry SC (2015) Hetero-trans-β-glucanase, an enzyme unique to *Equisetum* plants, functionalizes cellulose. Plant J 83:753–769. https://doi.org/10.1111/tpj.12935

Smith RC, Fry SC (1991) Endotransglycosylation of xyloglucans in plant cell suspension cultures. Biochem J 279:529–535. https://doi.org/10.1042/bj2790529

Steele NM, Sulová Z, Campbell P, Braam J, Farkaš V, Fry SC (2001) Ten isoenzymes of xyloglucan endotransglycosylase from plant cell walls select and cleave the donor substrate stochastically. Biochem J 355:671–679. https://doi.org/10.1042/bj3550671

Stratilová E, Ait-Mohand F, Řehulka P, Garajová S, Flodrová D, Řehulková H, Farkaš V (2010) Xyloglucan endotransglycosylases (XETs) from germinating nasturtium (*Tropaeolum majus*) seeds: Isolation and characterization of the major form. Plant Phys Biochem 48:207–215. https://doi.org/10.1016/j.plaphy.2010.01.016

Sulová Z, Baran R, Farkaš V (2003) Divergent modes of action on xyloglucan of two isoenzymes of xyloglucan endo-transglycosylase from *Tropaeolum majus*. Plant Phys Biochem 41:31–437. https://doi.org/10.1016/S0981-9428(03)00050-0

Thompson JE, Fry SC (2001) Restructuring of wall-bound xyloglucan by transglycosylation in living plant cells. Plant J 26:23–34. https://doi.org/10.1046/j.1365-313x.2001.01005.x

Thompson JE, Smith RC, Fry SC (1997) Xyloglucan undergoes interpolymeric transglycosylation during binding to the plant cell wall in vivo: evidence from 13C/3H dual labelling and isopycnic centrifugation in caesium trifluoroacetate. Biochem J 327:699–708. https://doi.org/10.1042/bj3270699

Vincken JP, York WS, Beldman G, Voragen AGJ (1997) Two general branching patterns of xyloglucan, XXXG and XXGC. Plant Phys 114:9–13. https://doi.org/10.1104/pp.114.1.9

Vissenberg K, Martinez-Vilchez IM, Verbelen JP, Miller JG, Fry SC (2000) In vivo colocalization of xyloglucan endotransglycosylase activity and its donor substrate in the elongation zone of *Arabidopsis* roots. Plant Cell 12:1229–1237. https://doi.org/10.1105/tpc.12.7.1229

York WS, van Halbeek H, Darvill AG, Albersheim P (1990) Structural analysis of xyloglucan oligosaccharides by ^{1}H-N.M.R. spectroscopy and fast-atom-bombardment mass spectrometry. Carbohydr Res 200:9–31. https://doi.org/10.1016/0008-6215(90)84179-X

York WS, Harvey LK, Guillen R, Albersheim P, Darvill AG (1993) Structural analysis of tamarind seed xyloglucan oligosaccharides using β-galactosidase digestion and spectroscopic methods. Carbohydr Res 248:285–301. https://doi.org/10.1016/0008-6215(93)84135-S

Zemková Z, Garajová S, Flodrová D, Řehulka P, Zelko I, Vadkertiová R, Farkaš V, Stratilová E (2012) Incorporation of β-(1,6)-linked glucooligosaccharides (pustulooligosaccharides) into plant cell wall structures. Chem Pap 66:14–820. https://doi.org/10.2478/s11696-012-0167-x

Affiliations

Barbora Stratilová[1,2] · Zuzana Firáková[1] · Jaroslav Klaudiny[1] · Sergej Šesták[1] · Stanislav Kozmon[1] · Dana Strouhalová[3] · Soňa Garajová[1] · Fairouz Ait-Mohand[1] · Ágnes Horváthová[1] · Vladimír Farkaš[1] · Eva Stratilová[1] · Maria Hrmova[4,5]

✉ Maria Hrmova
maria.hrmova@adelaide.edu.au

[1] Centre for Glycomics, Institute of Chemistry, Slovak Academy of Sciences, Dúbravská cesta 9, 84538 Bratislava, Slovakia

[2] Department of Physical and Theoretical Chemistry, Faculty of Natural Sciences, Comenius University, Mlynská dolina, 842 15 Bratislava, Slovakia

[3] Institute of Analytical Chemistry, Czech Academy of Sciences, v.v.i. Veveří, 60200 Brno, Czech Republic

[4] School of Life Sciences, Huaiyin Normal University, Huai'an 223300, China

[5] School of Agriculture, Food and Wine, and Waite Research Institute, Waite Research Precinct, University of Adelaide, Glen Osmond, SA 5064, Australia